Note that $exp\{x\}$ in this report denotes e^x

Evaluating the Accuracy and Efficiency of European Style Exotic Option Pricing in Markets with Dynamic Volatility Profiles

1. Introduction and Problem Statements

Traditional option pricing models, such as the Black-Scholes model, make specific assumptions about market behavior such as constant volatility and log-normal distribution of stock prices which do not hold for exotic options. Exotic options like Asian and lookback options have features that introduce path dependency and averaging, which present unique challenges for pricing. Furthermore, real markets often exhibit dynamic volatility, which can have a significant impact on the value of these complex derivatives.

This report delves into the complex valuation of Asian and Lookback options through a detailed comparative analysis of Monte Carlo simulations against vanilla options and analytical pricing formulas. It seeks to evaluate the efficacy and accuracy of Monte Carlo methods against traditional analytical models by examining option prices across various volatility settings and configurations. Furthermore, the research incorporates advanced uncertainty modeling techniques, including parametric and non-parametric approaches, to assess their impact on the pricing dynamics of Lookback options. By computing standard errors and analyzing the stability of results across multiple simulation runs, this study aims to provide insights into the robustness of simulation methods and their practical implications in financial modeling. Note that all options which are mentioned in this report are European style options. Thus, no early exercise is taken into account. Moreover, the analytical derivation of Asian option pricing formula has not been successful, further research is needed to complete the derivation.

Research Objectives:

1. Enhance of pricing accuracy: improve the accuracy of pricing models for Asian and lookback options by employing Monte Carlo simulations and analytical solutions. Traditional analytical models often assume ideal market conditions which may not hold under real-world market dynamics. This research investigates how closely Monte Carlo simulations can match or exceed the accuracy of these models in various market conditions.
2. Analysis of model sensitivity to volatility: Examine how changes in volatility affect the pricing of Asian and lookback options.
3. Evaluation of methodology robustness: Evaluate the robustness and reliability of Monte Carlo simulations by analyzing the stability of option prices across multiple simulation runs. Monte Carlo methods are powerful but can suffer from variance issues due to their stochastic nature. This research tries to quantify the stability and reliability of these simulations, providing insights into their practical application in financial modeling.

4. Uncertainty modelling in exotic option pricing: Apply both parametric and non-parametric uncertainty modelling techniques to study their effects on the pricing of lookback options specifically.
5. Practical financial applications: Translate theoretical findings into practical strategies and recommendations for portfolio managers and traders. This part of information can be found extensively under section 5.

2. Monte Carlo Simulation Process Development

2.1. Random Walk and Risk Neutrality

According to Wilmott (2007) and the given information, the fair value of an option is the present value of the expected payoff at expiry under a risk-neutral random walk for the underlying. Since the underlying asset we are investigating here is stock, and it is common to assume that stock price S_t follows the below random process in continuous time:

$$dS_t = \mu S_t dt + \sigma S_t dW_t^{\mathbb{P}}$$

, which is also called Geometric Brownian motion. The initial state is S_0, μ is the expected return of the stock, σ is the volatility of the stock returns, $W_t^{\mathbb{P}}$ represents a wiener process (or Brownian motion) over time interval $[0, T]$, which is under the real-world probability measure $\mathbb{P}$. However, this is not the risk neutral random walk for S_t.

To price derivatives, we prefer to work in a risk-neutral measure $\mathbb{Q}$ where all assets are expected tp grow at the risk free rate r. To swift from a real world measure $\mathbb{P}$ to a risk-neutral measure $\mathbb{Q}$, we can use Girsanov's theorem, which allows us to transform the Brownian motion $W_t^{\mathbb{P}}$ into a Brownian motion $W_t^{\mathbb{Q}}$ under the new measure $\mathbb{Q}$ and change the probability measure such that the discounted stock price becomes a martingale, then we can derive the equation of simulating underlying stock price by applying Euler Maruyama method.

The derivation steps of the solution of dS_t can be found in **Appendix A**. The solution is presented here directly:

$$S_t = S_0 e^{\left(\mu - \frac{1}{2}\sigma^2\right)t + \sigma W_t^{\mathbb{P}}}$$

Now, let's discount the underlying stock price $S_t^* = \frac{S_t}{B_t}$, where B_t denotes the risk free asset which follows the below dynamics:

$$dB_t = rB_t dt$$

The central idea behind the use of discounted stock prices stems from the necessity to adjust for the time value of money and to ensure that the pricing model is consistent with the principle of no-arbitrage. In the case of derivative pricing, the stock price itself represents a future cash flow, anticipated at the time of option expiry or at any future point when the stock might be sold. Therefore, the discounted stock price S_t^* is used to adjust the stock price to its present value, allowing for a consistent evaluation against other present-valued financial instruments.

Furthermore, the principle of no-arbitrage is central to risk neutral valuation. No-arbitrage conditions imply that there should be no possibility of making a risk-free profit through clever combinations of buying and selling in the market without investing capital or taking on risk. By converting to a risk-neutral measure (where the expected rate of return on all securities is the risk free rate r. Considering the discounted stock price, the essential idea is to normalize the returns of different securities to a common baseline, eliminating any arbitrage opportunities. This risk neutral world is not reflective of the real world probabilities but is a theoretical construct that facilitates the valuation of derivatives in a mathematically tractable and economically rational way.

Let's rearrange dB_t and obtain the below Ordinary Differential Equation:

$$\frac{dB_t}{B_t} = rdt$$

Integrate both sides, and the result can be obtained:

$$\int_0^t \frac{1}{B_u} dB_u = \int_0^t r\, ds$$

$$\ln(B_t) - \ln(B_0) = rt$$

$$B_t = B_0 e^{rt}$$

Going back to S_t^*, the below process can be obtained:

$$S_t^* = \frac{S_t}{B_t} = \frac{S_0 e^{\left(\mu - \frac{1}{2}\sigma^2\right)t + \sigma W_t^{\mathbb{P}}}}{B_0 e^{rt}} = S_0^* e^{\left(\mu - r - \frac{1}{2}\sigma^2\right)t + \sigma W_t^{\mathbb{P}}}$$

Define a function $f\left(t, W_t^{\mathbb{P}}\right)$, and let $f\left(t, W_t^{\mathbb{P}}\right) = S_t^*$:

$$f\left(t + dt, W_t^{\mathbb{P}} + dW_t^{\mathbb{P}}\right) = f\left(t, W_t^{\mathbb{P}}\right) + \frac{\partial f}{\partial t} dt + \frac{\partial f}{\partial W_t^{\mathbb{P}}} dW_t^{\mathbb{P}} + \frac{1}{2}\frac{\partial^2 f}{\partial t^2}(dt)^2 + \frac{1}{2}\frac{\partial^2 f}{\partial {W_t^{\mathbb{P}}}^2}\left(dW_t^{\mathbb{P}}\right)^2$$

$$= f\left(t, W_t^{\mathbb{P}}\right) + \frac{\partial f}{\partial t} dt + \frac{\partial f}{\partial W_t^{\mathbb{P}}} dW_t + \frac{1}{2}\frac{\partial^2 f}{\partial {W_t^{\mathbb{P}}}^2} dt$$

As a result:

$$df\left(t, W_t^{\mathbb{P}}\right) = \left(\frac{\partial f}{\partial t} + \frac{1}{2}\frac{\partial^2 f}{\partial {W_t^{\mathbb{P}}}^2}\right)dt + \frac{\partial f}{\partial W_t^{\mathbb{P}}}dW_t^{\mathbb{P}}$$

By finding the partial derivatives of function f:

$$\frac{\partial f}{\partial t} = \frac{\partial S_t^*}{\partial t} = \left(\mu - r - \frac{1}{2}\sigma^2\right)S_0^* e^{\left(\mu - r - \frac{1}{2}\sigma^2\right)t + \sigma W_t^{\mathbb{P}}}$$

$$\frac{\partial f}{\partial W_t} = \frac{\partial S_t^*}{\partial W_t} = \sigma S_0^* e^{\left(\mu - r - \frac{1}{2}\sigma^2\right)t + \sigma W_t^{\mathbb{P}}}$$

$$\frac{\partial^2 f}{\partial W_t^2} = \frac{\partial^2 S_t^*}{\partial W_t^2} = \sigma^2 S_0^* e^{\left(\mu - r - \frac{1}{2}\sigma^2\right)t + \sigma W_t^{\mathbb{P}}}$$

Substitute them back into the differential equation:

$$dS_t^* = \left[\left(\mu - r - \frac{1}{2}\sigma^2\right)S_0^* e^{\left(\mu - r - \frac{1}{2}\sigma^2\right)t + \sigma W_t^{\mathbb{P}}} + \frac{1}{2}\,\sigma^2 S_0^* e^{\left(\mu - r - \frac{1}{2}\sigma^2\right)t + \sigma W_t^{\mathbb{P}}}\right]dt$$
$$+ \sigma S_0^* e^{\left(\mu - r - \frac{1}{2}\sigma^2\right)t + \sigma {W_t^{\mathbb{P}}}_t} dW_t^{\mathbb{P}}$$

$$= \left[(\mu - r)S_0^* e^{\left(\mu - r - \frac{1}{2}\sigma^2\right)t + \sigma W_t^{\mathbb{P}}} + S_0^* e^{\left(\mu - r - \frac{1}{2}\sigma^2\right)t + \sigma W_t^{\mathbb{P}}}\right]dt + \sigma S_0^* e^{\left(\mu - r - \frac{1}{2}\sigma^2\right)t + \sigma W_t^{\mathbb{P}}} dW_t^{\mathbb{P}}$$

Given that $S_t^* = S_0^* e^{\left(\mu - r - \frac{1}{2}\sigma^2\right)t + \sigma W_t}$, the below new SDE for discounted stock price S_t^* will be obtained:

$$dS_t^* = (\mu - r)S_t^* dt + \sigma S_t^* dW_t^{\mathbb{P}}$$

Under measure $\mathbb{P}$, dS_t^* is not a martingale, to make dS_t^* a martingale, it is necessary to find a probability measure for dW_t such that:

$$(\mu - r)S_t^* dt = 0$$

Therefore, define a new probability measure $\mathbb{Q}$, also being called risk neutral probability measure, and under $\mathbb{Q}$, $\mu = r$, such that dS_t^* will be a martingale:

$$dS_t^* = \sigma S_t^* dW_t^{\mathbb{Q}}$$

Girsanov theorem and Radon Nikodym derivatives will allow us to find a relationship such that:

$$\mathbb{Q}(\mathcal{A}) = \int_{\mathcal{A}} \Lambda \, d\mathbb{P}$$

Now, define a stochastic process θ_t that is adapted to the filtration by $W_t^{\mathbb{P}}$, if the below Novikov condition is satisfied:

$$\mathbb{E}^{\mathbb{P}}\left[\exp\left\{\frac{1}{2}\int_0^T \theta_s^2 \, ds\right\}\right] < \infty$$

Girsanov theorem will give the below relationship if $\mathbb{Q}$ and $\mathbb{P}$ are equivalent probability measures (proof is shown in **Appendix B**):

$$\frac{d\mathbb{Q}}{d\mathbb{P}} = \Lambda = \exp\left\{-\int_0^t \theta_s \, dW_s^{\mathbb{P}} - \frac{1}{2}\int_0^t \theta_s^2 \, ds\right\}$$

$$W_t^{\mathbb{Q}} = W_t^{\mathbb{P}} - \int_0^t \theta_s \, ds$$

Therefore, $W_t^{\mathbb{Q}}$ will be a standard Brownian motion. Now let $\theta_t = \frac{\mu - r}{\sigma}$, where r is the risk free interest rate and μ is the drift under $\mathbb{P}$ probability measure. (The choice of θ_t is made such that under probability measure $\mathbb{Q}$, the expected return of the stock discounted at risk free interest rate will be a martingale).

Let's start again with the below SDE under probability measure $\mathbb{P}$:

$$dS_t = \mu S_t dt + \sigma S_t dW_t^{\mathbb{P}}$$

Knowing that

$$W_t^{\mathbb{P}} = W_t^{\mathbb{Q}} + \int_0^t \theta_s \, ds = W_t^{\mathbb{Q}} + \int_0^t \frac{\mu - r}{\sigma} ds$$

Take differentials from both sides:

$$dW_t^{\mathbb{P}} = dW_t^{\mathbb{Q}} + d\int_0^t \frac{\mu - r}{\sigma} ds = dW_t^{\mathbb{Q}} + \frac{\mu - r}{\sigma} dt$$

Substitute it back into the original price dynamics dS_t:

$$dS_t = \mu S_t dt + \sigma S_t \left(dW_t^{\mathbb{Q}} + \frac{\mu - r}{\sigma} dt\right)$$

$$= \mu S_t dt + \sigma S_t dW_t^{\mathbb{Q}} + \sigma S_t \frac{\mu - r}{\sigma} dt$$

$$= \mu S_t dt + \sigma S_t dW_t^{\mathbb{Q}} + S_t(\mu - r) dt$$

$$= (2\mu - r) S_t dt + \sigma S_t dW_t^{\mathbb{Q}}$$

From the above derivation for the discounted price dynamics, under risk neutral probability measure, $\mu = r$, as a result:

$$dS_t = (2r - r) S_t dt + \sigma S_t dW_t^{\mathbb{Q}} = r S_t dt + \sigma S_t dW_t^{\mathbb{Q}}$$

2.2. Euler Maruyama Scheme

The Euler Maruyama methods is a numerical scheme used to approximate solutions to stochastic differential equations (SDEs). This scheme replies on the discretization of the continuous time process

into small time steps δt, and it approximates the solution of dS_t under $\mathbb{Q}$ measure at discrete time steps as below:

$$S_{t+\delta t} - S_t = \delta S_t = rS_t\delta t + \sigma S_t \delta W_t$$

The increments of Wiener process δW_t is discretized through dividing the total time T into small equal intervals $\delta t = \frac{T}{N}$, over each interval, the increment of Wiener process can be modelled as $\sqrt{\delta t}Z$, where Z is a standard normal random variable following the $\mathcal{N}(0,1)$ distribution. This modelling is grounded in the properties of Brownian motion, where the variance of the process over a time interval δt is directly proportional to δt, hence the scaling by $\sqrt{\delta t}$. The proof of the convergence of $\sqrt{\delta t}Z$ into a continuous Wiener process in shown in the **Appendix C**. As a result, the Euler Maruyama scheme approximates dS_t in the below manner:

$$\delta S_t = rS_t\delta t + \sigma S_t\sqrt{\delta t}\, Z$$

The path simulating algorithm (see <class PathSimulator>) demonstrates how Euler Maruyama scheme is applied to simulate the stock prices, as described by the above SDE. The <def generate_path> function follows the exact same logic as δS_t shows. The variable <steps> in the code combines the drift and diffusion terms of the process. Note that the cumulative sum of the <steps> is captured by the variable <path> and is exponentiated and then scaled by the initial stock price S_0 following the logic of the below solution of the SDE dS_t:

$$S_t = S_0 e^{\left(r-\frac{1}{2}\sigma^2\right)t+\sigma W_t^{\mathbb{Q}}}$$

The derivation of this solution follows the same logic as the steps shown in **Appendix A**. The initial stock price S_0 is inserted and initialized at the beginning of the simulation.

2.3. Monte Carlo Simulation

Monte Carlo simulation is a computational algorithm that uses repeated random sampling to obtain numerical results. To implement Monte Carlo simulation together with Euler-Maruyama scheme, it is necessary to simulate multiple paths of S_T using the formula δS_t developed in section 2.2.

The ultimate goal is to estimate the below expectation:

$$\mathbb{E}[e^{-rT}S_T] = \int e^{-rT}S_T(\omega)\mathbb{P}(d\omega)$$

$S_T(\omega)$ represents the stock price at time T under a particular realization ω of the stochastic process. Given the discretized paths from the Euler-Maruyama methods, $\mathbb{E}[e^{-rT}S_T]$ can be estimated by averaging the outcomes of $e^{-rT}S_T$ over a large number M of simulated paths. Let $\left\{S_T^{(1)}, S_T^{(2)}, \dots, S_T^{(M)}\right\}$

be the final stock prices from M simulated paths, the Monte Carlo estimate for the expected value is given by:

$$\hat{I} = \frac{1}{M}\sum_{i=1}^{M} e^{-rT} S_T^{(i)}$$

The accuracy of the Monte Carlo estimate $\hat{I}$ improves with increasing M due to the law of large numbers, which states that $\hat{I}$ converges to $\mathbb{E}[e^{-rT}S_T]$ as $M \to \infty$.

Monte Carlo simulation is highly advantageous for pricing path-dependent exotic options and other high-dimensional problems because it naturally handles multiple dimensions and complex path dependencies without the need for simplifications inherent in other numerical methods. This flexibility allows it to model scenarios that are otherwise intractable with deterministic methods. However, Monte Carlo simulation can be computationally intensive, often requiring a large number of simulations to achieve acceptable accuracy, which can be significantly time-consuming. Moreover, the accuracy of Monte Carlo estimates can be sensitive to the quality of the random number generation and the specific method of variance reduction employed.

3. European Style Asian and Lookback Options

In this study, European style Asian and Lookback options will be exclusively focused to simplify valuation by avoiding the complexity of early exercise inherent in American options. For American style options which might involve early exercises, the details of the payoff on early exercise have to be well defined, however, it will be very challenging and Monte Carlo simulation method will not be applicable.

To focus on European style options reflects the predominant market products and ensures analytical tractability. Moreover, by concentrating on these options, the study also aligns with the practical and educational needs of financial professionals, providing a solid foundation for understanding more complex derivatives within financial engineering and risk management contexts.

3.1. Asian Options

Asian options are one of the strongly path-dependent options whose terminal payoff depends on some form of averaging of the underlying asset's prices over a specified period. This period could cover the entire life of the option or just a part of it.

Denote A_T as some form of averaging, which is calculated at the end of the averaging period, S_u as the asset price over the time period $[0, t]$, K as the predetermined strike price at the initiation of the contract, the terminal payoff of Asian Options under different configurations can be defined as:

Floating Strike Call	Floating Strike Put	Fixed Strike Call	Fixed Strike Put
$\max(S_T - A_T, 0)$	$\max(A_T - S_T, 0)$	$\max(A_T - K, 0)$	$\max(K - A_T, 0)$

In this report, both of continuously monitored arithmetic and geometric averaging methods across the above four different configurations will be discussed, the discrete averaging methods will be discarded for the reason of convergence. Denote S_{t_i} as the asset price at discrete time t_i, where $i = 1,2,\dots,n$. In the limit $n \to \infty$, the discrete period sampled averages become the continuous sampled averages (See the proof in **Appendix D**). Therefore, continuous averaging methods will be used in this report. It also simplifies the calculations and is more natural for models driven by continuous stochastic processes.

Under continuous geometric averaging methods, we define the form of averaging $A_t, 0 \le t \le T$ as:

$$A_t = \exp\left\{\frac{1}{t}\int_0^t \ln S_u \, du\right\}$$

As a result we have the expectation forms of payoffs for fixed and floating Strike call options are:

$$C_{fixed}(S,t) = e^{-r(T-t)}\mathbb{E}^{\mathbb{Q}}\left[\max\left(\exp\left\{\frac{1}{t}\int_0^t \ln S_u \, du\right\} - K, 0\right)|S_t = S\right]$$

$$C_{float}(S,t) = e^{-r(T-t)}\mathbb{E}^{\mathbb{Q}}\left[\max\left(S_T - \exp\left\{\frac{1}{t}\int_0^t \ln S_u \, du\right\}, 0\right)|S_t = S\right]$$

The put payoffs can be defined similarly based on the table above.

Under continuous arithmetic averaging methods, we define the form of averaging A_T as:

$$A_T = \frac{1}{T}\int_0^T S_t dt$$

The terminal payoff for a fixed strike call option can be defined by::

$$\begin{aligned} C_{fixed}(S,t) &= e^{-r(T-t)}\mathbb{E}^{\mathbb{Q}}[\max(A_T - K, 0)] \\ &= e^{-r(T-t)}\mathbb{E}^{\mathbb{Q}}\left[\max\left(\frac{1}{T}\int_0^T S_t dt - K, 0\right)\right] \\ &= e^{-r(T-t)}\mathbb{E}^{\mathbb{Q}}\left[\max\left(\frac{1}{T}\int_0^t S_u du - K + \frac{1}{T}\int_t^T S_u du, 0\right)\right] \\ &= \frac{S_t}{T}e^{-r(T-t)}\mathbb{E}^{\mathbb{Q}}\left[\max\left(\frac{t\int_0^t S_u du - KT}{S_t} + \int_t^T \frac{S_u}{S_t} du, 0\right)\right] \end{aligned}$$

The payoff expectations under other configurations can be defined similarly as above.

3.2. Lookback Options

Lookback Options are another strongly path dependent options whose payoffs depend on the maximum or minimum of the underlying asset price obtained over a certain period of the time, usually defined as

lookback period in academia. This study first considers lookback options where lookback period is taken to be the whole life of the option. Let T denote the time of the expiration of the option, and $[0, T]$ be the lookback period. Denote the minimum value (m_0^T) and maximum value (M_0^T) of the underlying stock price realized from 0 to expiration T as:

$$m_0^T = \min_{0 \le t \le T} S_t$$

$$M_0^T = \max_{0 \le t \le T} S_t$$

Such definition also implicitly implies continuous monitoring of the asset price. Similar to Asian options, lookback options can also be classified into two types: fixed strike and floating strike. According to Wilmott (2007) and Kwok (2008), a floating strike lookback call gives the holder the right to buy at the lowest realized price while a floating strike lookback put allows the holder to sell at the highest realized price over the lookback period. Based on definition, the relationship of $M_0^T \geq S_T \geq m_0^T$ should hold, therefore, the holder of a floating strike lookback option always exercises. The respective terminal payoff of the floating strike lookback call and put are:

Floating Strike Call	Floating Strike Put
$\max(S_T - m_0^T, 0) = S_T - m_0^T$	$\max(M_0^T - S_T, 0) = M_0^T - S_T$

Furthermore, fixed strike lookback call option is a call option on the maximum realized price. The terminal payoff is

$$\max(M_0^T - K, 0)$$

A fixed strike lookback put option is a put option on the minimum realized price, and the respective terminal payoff is

$$\max(K - m_0^T, 0)$$

Given fixed strike lookback call option as an example, under risk neutral probability measure, the value of the option can be defined as:

$$C_{fixed}(S, t) = e^{-r(T-t)} \mathbb{E}^{\mathbb{Q}}[\max(M_0^T - K, 0)]$$

Under the risk neutral probability measure, the value of the floating strike lookback call option can be defined as:

$$C_{fixed}(S, t) = e^{-r(T-t)} \mathbb{E}^{\mathbb{Q}}[\max(S_T - m_0^T, 0)] = e^{-r(T-t)} \mathbb{E}^{\mathbb{Q}}[S_T - m_0^T]$$

$$= e^{-r(T-t)} \mathbb{E}^{\mathbb{Q}}\left[S_T - \min_{0 \le t \le T} S_t\right]$$

The fixed strike and floating strike lookback put options pricing formulas follow the similar logic.

4. Algorithm Design

The Python algorithm is designed in an Object-Oriented Pattern, structured to modularly handle various option pricing simulations using the Monte Carlo method. The core of the system is based on classes that summarizes specific functionalities, such as configuration management <class Config>, path simulation <class PathSimulator>, and option pricing for different types <class AsianOptionPricer>, <class LookbackOptionPricer>. Each class is responsible for a distinct aspect of the simulation process, ensuring that the code is both reusable and maintainable. The Config class, for instance, initializes and updates simulation parameters, while the <class PathSimulator> generates stochastic paths influenced by defined drift and diffusion terms, which are essential for simulating asset price movements over time.

Furthermore, the <class SimulationEngine> arranges the overall simulation workflow, managing multiple simulations and aggregating results. It utilizes the<class PathSimulator> to generate multiple paths and then passes these to the appropriate price objects based on the option type being evaluated. This class significantly simplifies the process of running extensive simulations and allows for easy extensions, such as varying volatility, strike prices, or the maturity of options. Through gathering the simulation logic within this central engine, the system enhances code readability and scalability, facilitating future expansions or modifications to include additional types of financial instruments or more complex pricing algorithms.

5. Comparative Analysis of Monte Carlo Simulated Prices

5.1. Comparison of Prices across Different Volatilities for Asian Options

Table 1 displays the results of Monte Carlo simulated prices for Asian and Lookback options across varying volatilities and strike prices with 10,000 seeds. These findings are also compared against the Black Scholes model employed for vanilla options. Note that the averaging period of the Asian options and lookback period of the Lookback periods are all the whole life of the options.

		Asian Call Options				Asian Put Options				Lookback Call		Lookback Put		Vanilla	
Strike	Sigma	Arithmetic Fixed Strike	Arithmetic Floating Strike	Geometric Fixed Strike	Geometric Floating Strike	Arithmetic Fixed Strike	Arithmetic Floating Strike	Geometric Fixed Strike	Geometric Floating Strike	Fixed Strike	Floating Strike	Fixed Strike	Floating Strike	Black Scholes Call	Black Scholes Put
95	0.05	6.97	0.33	7.19	0.32	0.00	2.74	0.00	2.74	11.56	6.86	0.12	1.90	9.67	0.04
100		2.70	0.33	2.74	0.31	0.29	2.63	0.31	2.70	7.18	6.53	1.91	1.95	5.28	0.41
105		0.37	0.29	0.27	0.31	2.84	2.80	2.74	2.63	2.85	6.74	6.64	2.00	2.05	1.93
95	0.2	8.98	3.38	8.67	3.32	1.57	5.83	1.68	5.66	23.13	17.28	7.73	14.03	13.35	3.71
100		6.02	3.05	5.91	3.34	3.45	5.44	3.27	5.28	18.48	16.67	11.74	13.76	10.45	5.57
105		3.37	3.50	3.42	3.46	5.70	5.89	6.14	5.57	14.35	16.20	16.70	13.39	8.02	7.90
95	0.3	10.35	5.32	10.62	5.76	3.22	7.18	3.62	6.77	31.64	22.49	13.77	21.66	16.80	7.17
100		8.28	5.39	7.86	5.64	5.84	7.62	5.94	7.12	27.98	22.83	18.15	22.42	14.23	9.35
105		5.67	5.84	5.01	5.74	7.75	8.34	8.12	7.61	22.90	23.20	22.38	22.74	11.98	11.86
95	0.5	14.07	10.47	14.12	10.44	7.72	12.63	8.21	11.69	47.81	33.03	25.08	41.19	23.98	14.35
100		13.24	9.46	11.17	10.51	9.80	11.76	10.87	11.66	45.53	33.04	30.02	41.81	21.79	16.92
105		9.74	10.25	9.27	10.34	12.63	11.76	13.64	11.37	42.28	32.85	34.48	42.45	19.79	19.67
95	0.6	15.96	11.25	15.23	12.99	9.20	15.55	11.10	12.10	62.03	41.92	30.12	46.78	27.57	17.94
100		13.87	11.63	13.11	12.33	12.20	12.52	14.46	13.03	56.25	39.98	35.56	51.28	25.52	20.65
105		12.37	11.42	11.85	13.27	13.86	13.37	16.87	12.39	50.74	38.76	38.07	50.83	23.63	23.51
95	0.8	18.07	16.58	17.93	18.78	13.61	20.75	16.20	14.85	83.39	47.58	38.55	72.19	34.63	24.99
100		20.60	16.08	15.62	18.52	16.39	20.15	18.32	14.05	77.05	48.25	43.43	72.10	32.82	27.94
105		15.52	17.50	14.73	19.71	18.73	18.63	22.07	14.47	73.44	45.77	48.90	71.97	31.13	31.01
95	1	25.63	20.60	19.17	23.72	17.57	20.82	21.01	17.85	105.80	57.96	48.43	96.63	41.44	31.80
100		21.69	20.71	19.79	22.60	19.90	22.90	23.20	20.68	104.05	60.09	53.80	98.43	39.84	34.96
105		20.23	20.93	16.36	23.88	24.23	21.39	27.59	18.45	90.63	61.45	58.16	96.26	38.33	38.21

Table 1 – Monte Carlo Simulation Results for Asian and Lookback Options under Various Configurations

For Asian options, the results indicate a clear trend of price increase with volatility. For instance, with a volatility $\sigma = 0.05$, the price of an arithmetic Asian call option with a fixed strike of 100 is approximately 2.7, which escalates to around 6.02 when the volatility increases to 0.2. This pattern underlines the fundamental theory that higher volatility enhances the value of options due to increased uncertainty and the stock's potential to reach favorable strike conditions.

A comparison between arithmetic and geometric averaging methods also presents significant pricing differentials. Specifically, the arithmetic fixed strike call priced at approximately 8.98 under $\sigma = 0.2, K = 95$ surpasses its geometric counterpart, which is priced around 8.67. The arithmetic average is more sensitive to transient spikes and dips in asset prices, whereas the geometric average, being multiplicative, tends to dilute the impact of extreme values, leading to a potentially lower calculated average and thus a lower option price. As can be shown from the **Table 1** and **the Figure 1** below, this effect is more significant when volatility of the underlying is high ($\sigma = 0.8$ for example), signifying greater likelihood of more extreme values in the price path. Therefore, from a speculative perspective, arithmetic Asian options might offer higher returns than geometric ones because they respond more sensitively to price changes. If a trader speculates that the underlying asset will experience significant

price variations within the averaging period, the arithmetic average will reflect these changes more markedly, potentially offering greater gains if the speculation is correct.

Furthermore, the results also illustrate a pricing distinction between fixed and floating strike options. Floating strike options are consistently priced lower across both call and put configurations, which is related to the mechanism that the strike price in floating options being set at the average asset price over the life of the option (recall the payoff definition of floating strike Asian options above). This method typically results in a strike price that is more aligned with the prevailing market conditions at the time of exercise, reducing the option's intrinsic value volatility and, consequently, its price. For example, an arithmetic floating strike call option at $\sigma = 0.2, K = 95$ is priced at approximately 3.38, substantially less than its fixed strike equivalent (also can be viewed in **Figure 1**, the orange bar is significantly shorter than the blue one). This reduced pricing makes floating strike options appealing for aligning closely

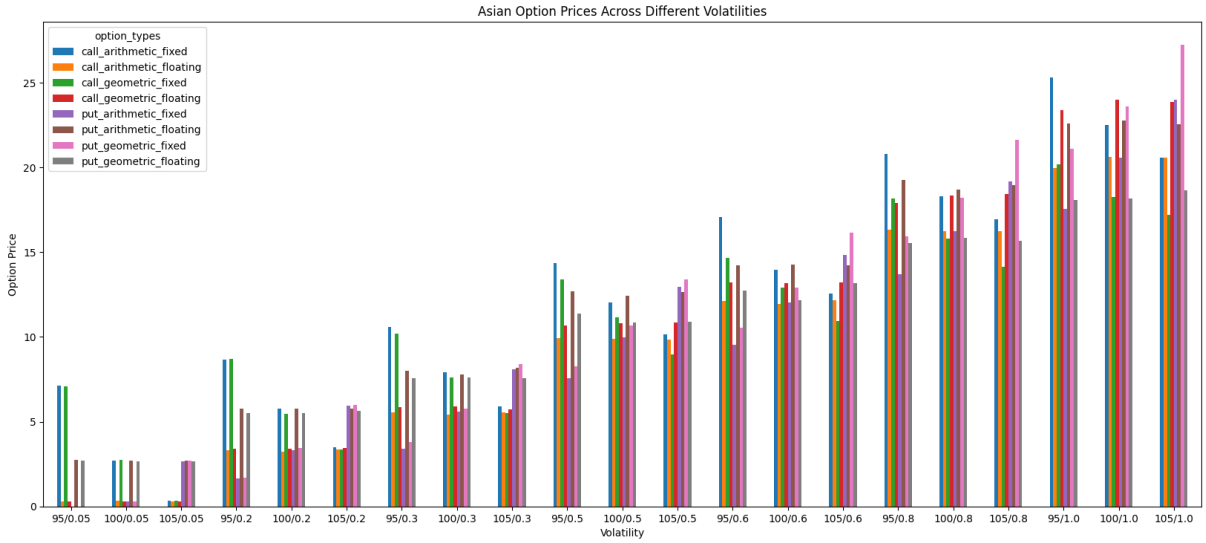

Figure 1 – Asian Option Prices across Different Configurations

with prevailing market conditions without overpaying. Therefore, for investors or hedgers looking for cost-effective options that offer protection or profit opportunities closely aligned with actual market averages, floating strike options may be more appealing than fixed strike options, which carry a premium for their predictability and stability.

5.2. Comparison of Prices across Different Volatilities for Lookback Options

Lookback Options, known for their flexibility in selecting the most favorable execution price, demonstrate a higher pricing compared to both of Asian and vanilla options, as it effectively provides an optionality on the optimal timing of exercise, which is particularly valuable in volatile markets. Given their higher costs, lookback options might be rather attractive in markets where high volatility is anticipated, or where investors wish to maximize returns on investments with inherently unpredictable price movements.

This premium reflects their added value in volatile markets. For instance, a fixed strike lookback call at $\sigma = 0.2, K = 95$ is valued at 23.13 (see **Table 1**), illustrating the premium investors pay for the advantage of selecting the optimal exercise time.

The influence of volatility on lookback options is also marked, with prices increasing as volatility rises. The ability to exploit maximum or minimum prices during the option's life becomes more profitable as these extremes broaden with higher volatility. This is better visualized in **Figure 2**, and can be explained by their feature that allows capitalizing on the maximum or minimum prices reached. As volatility increases, the range of potential maximum or minimum prices expands, thus, increasing the expected payoff and the cost of the option. These options should be suitable for scenarios where investors anticipate significant price movements but are unsure of the direction.

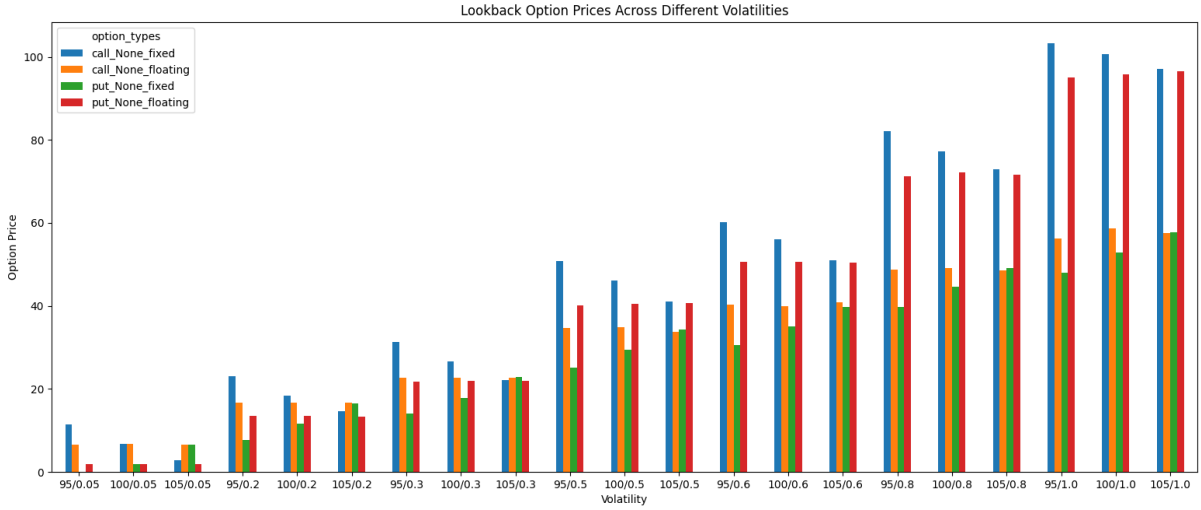

Figure 2 – Lookback Option Prices across Different Configurations

Similar to Asian options, fixed strikes are generally more expensive than floating strikes, due to the certainty and potentially advantageous positioning they offer against market forecasts. Investors can use fixed strike lookback options to maximize returns in environments where the underlying asset is expected to move significantly past the strike price. This can be useful in bullish or bearish markets where the direction is somewhat predictable but the magnitude of the movement is uncertain. Floating strike lookback options adjust the strike price to the lowest (for puts) or highest (for calls) price of the underlying asset during the life of the option. It is reasonable that these options can be more cost-effective compared to fixed strikes as they reduce the risk premium investors have to pay. The strike price adjustment mechanism aligns more closely with the underlying stock's actual performance, potentially lowering the cost of the option compared to a fixed strike option with a misaligned strike price.

5.3. Impact of Varying Strike Prices on Option Pricing

Strike price variations exhibit a clear impact on the pricing of fixed strike Asian options across both arithmetic and geometric averaging methods. As observed in the **Figure 1** and **Table 1**, the pricing sensitivity to strike price increases in obvious. For example, with a low volatility of $\sigma = 0.05$, the arithmetic fixed strike Asian call option decreases sharply in price from approximate 6.97 at $K = 95$ to approximately 0.37 at $K = 105$. This trend suggests that higher strike prices significantly reduce the likelihood of profitable execution for buyers, hence lowering the option price.

From a financial market perspective, as the strike price increases, the likelihood that the option will end up in-the-money at expiration decreases. In low volatility conditions, where large price swings are less likely, the chance that the asset price will surpass a higher strike price diminishes, therefore, reducing the option's intrinsic value and consequently its price.

Similar trends are also noted for geometric averaging Asian options, however, the decrease in prices with increase strikes is generally less steep comparing to arithmetic averaging Asian options. Especially when the market is volatile, when $\sigma = 1$, the decrease in price associated with increase in fixed strikes geometric averaging Asian call options is less compared to arithmetic averaging options.

In examining the floating strike Asian options, it's observed that prices remain relatively unaffected by increases in the predefined strike settings for both geometric and arithmetic averaging methods. This behavior aligns with expectations, as the mechanism defining the strike price in floating strike options differs fundamentally from that in fixed strike options. In floating strike configurations, the strike price is determined by the average price of the underlying asset over the option's life, rather than being preset at initiation. This intrinsic adjustment allows the strike price to dynamically align with market conditions, thereby mitigating the sensitivity to initial strike price settings. As a result, floating strike options provide a more stable pricing structure that adapts to market changes, making them particularly valuable for investors seeking options that reflect real-time asset performance without the volatility typically associated with fixed strikes.

Additionally, for fixed strike lookback options, they exhibit a higher sensitivity to strike prices, which is similar to the observations from Asian options. This pattern underscores the increased risk and reduced flexibility associated with fixed strikes as the strike price rises. Meanwhile, floating strike lookback options are less affected by changes in the strike price. This stability is also attributed to the option's mechanism that adjusts the strike price to most favorable market conditions throughout its terms.

5.4. Visualizing Option Dynamics: Fixed Strike Options

Figure 3 generated from the Monte Carlo simulations effectively illustrate the intricate interplay between volatility across different levels: volatility, spot price, and time to maturity in determining option prices. Note that Figure 3 presents the cases of volatility $\sigma = 0.2$ and $\sigma = 0.8$, and only for

arithmetic Asian call options (first row) and geometric Asian call Options (second row) These plots reveal a pronounced sensitivity of option prices to changes in volatility. As volatility increases, the range and variability of option prices expand substantially. This pattern aligns with established financial theories that posit higher volatility as enhancing the underlying asset's potential to reach favorable price levels, thereby increasing the option's potential payoff. Additionally, the comparison between arithmetic and geometric averaging methods shows distinct behaviors: arithmetic averaging captures higher peaks and more price variability, reflecting acute sensitivity to price spikes, whereas geometric averaging exhibits a smoother surface and lower peaks, indicating reduced responsiveness to rapid price changes.

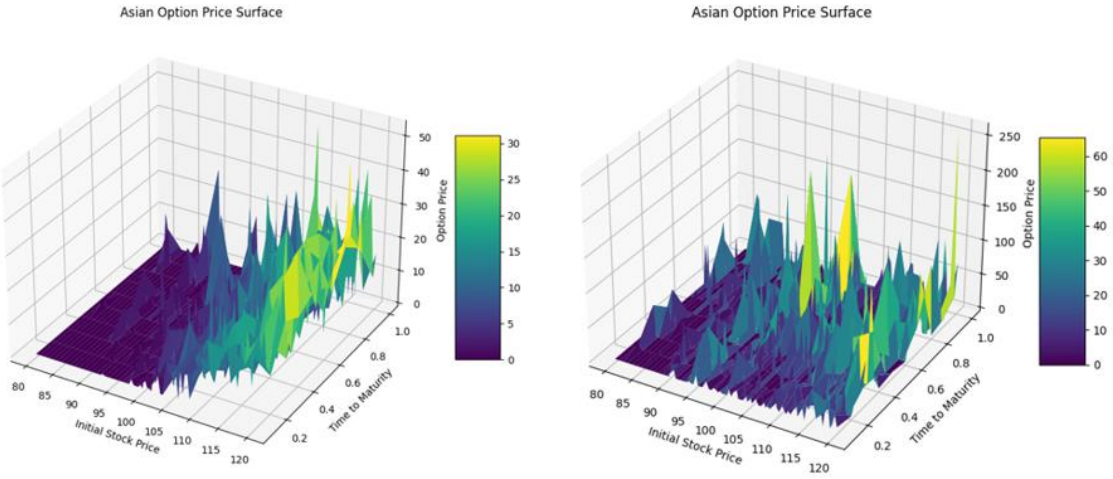

Arithmetic Averaging Fixed Strike Asian call options with strike = 100, and vol = 0.2 (left), vol = 0.8 (right)

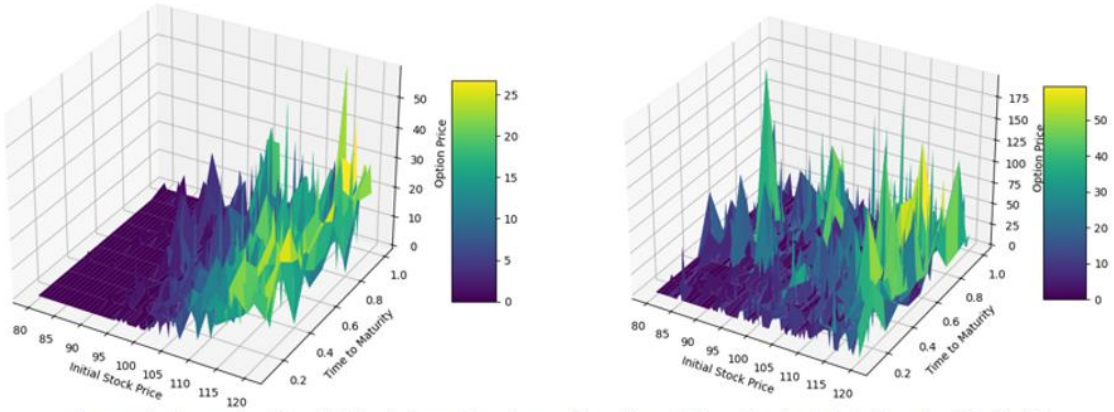

Geometric Averaging Fixed Strike Asian call options with strike = 100, and vol = 0.2 (left), vol = 0.8 (right)

Figure 3 – Three Dimensional Plots: Option Value, Spot Prices, Time to Matutiry

The dimension of time to maturity also plays a crucial role, with longer maturities typically associated with higher prices due to the increased likelihood of achieving favorable conditions. However, as maturity approaches, a decay in option prices is observed, highlighting the temporal depreciation of option value.

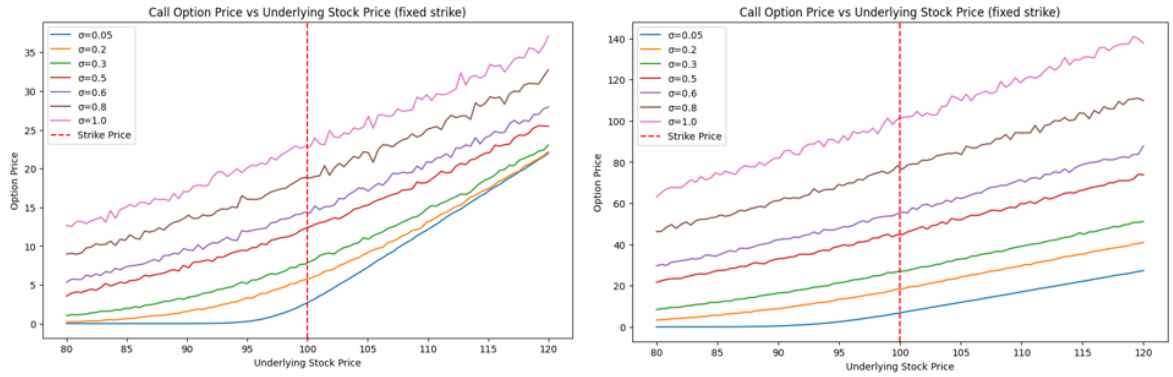

Arithmetic Fixed Strike Asian Call Option $K = 100$ Fixed Strike Lookback Call Option $K = 100$

Figure 4 – Fixed Strike Call Option prices vs. Spot Prices

Figure 4 depicting fixed strike call option prices as a function of the underlying spot price for different volatility scenarios further elucidate the behavior of options under varying market conditions. Together with **Figure 3**, the fluctuations are captured in the option prices themselves across different spot prices when the volatility is high.

This observation contrasts the behavior typically expected from plain vanilla options. However, this also shows that Asian options are distinct due to their averaging mechanism over the option's life, which affects the payoff. In fixed-strike Asian options, the payoff is dependent on the average price of the underlying asset rather than the price at maturity. This averaging can lead to more volatile option price paths in simulations, as the average can be heavily influenced by short-term spikes or drops in the asset's price, contributing to greater variability in the option's value prior to maturity.

Lookback options, characterized by their feature allowing the holder to "look back" at the price history of the underlying asset and select the most favorable exercise price, exhibit unique price behaviors as shown in the right panel of **Figure 4**. The ability of these options to minimize downside risk and maximize upside potential is vividly depicted as the option price increases across higher volatility profiles. This trait stems from the option's design to capitalize on the optimal price achieved during the life of the option, rather than being limited to the price at maturity or an average price.

Unlike fixed-strike Asian options, where the option's sensitivity to price fluctuations is somewhat moderated by the averaging mechanism, Lookback options directly benefit from high peaks in asset prices, which can be seen from the y-axis of the right panel figure in **Figure 4**. While Asian options exhibit increased volatility in their pricing due to averaging, Lookback options show even greater sensitivity to changes in the underlying asset's price as they always have the potential to exercise at the best observed price.

The concept of moneyness in Lookback options is inherently dynamic. As the underlying asset's price surpasses the strike price (indicated by the vertical red line in the plot), the options quickly move in-the-

money, reflecting their intrinsic advantage. **Figure 4** clearly shows a steep increase in option prices past the strike price across all volatility levels, indicating rapid gains in intrinsic value. This behavior is particularly pronounced in high-volatility scenarios where the chances of achieving a price much higher than the strike price are increased.

To summarize, lookback options generally exhibit higher volatility sensitivities than Asian options. For fixed strike lookback options, they are particularly sensitive to volatility because the payoff maximizes based on the highest or lowest asset prices reached during the option's life. Higher volatility increases the range of potential extreme values, which significantly impacts the option's value. The fixed strike version magnifies this effect since the strike price remains constant, and the benefit from extreme values becomes more pronounced. For floating strike lookback options, while also sensitive to volatility, the floating strike versions adjust the strike price based on the asset's historical performance, somewhat mitigating the direct impact of increased volatility. However, they still benefit from wider price ranges introduced by higher volatility, although to a leaser extend than their fixed strike counterparts.

5.5. Visualizing Option Dynamics: Floating Strike Options

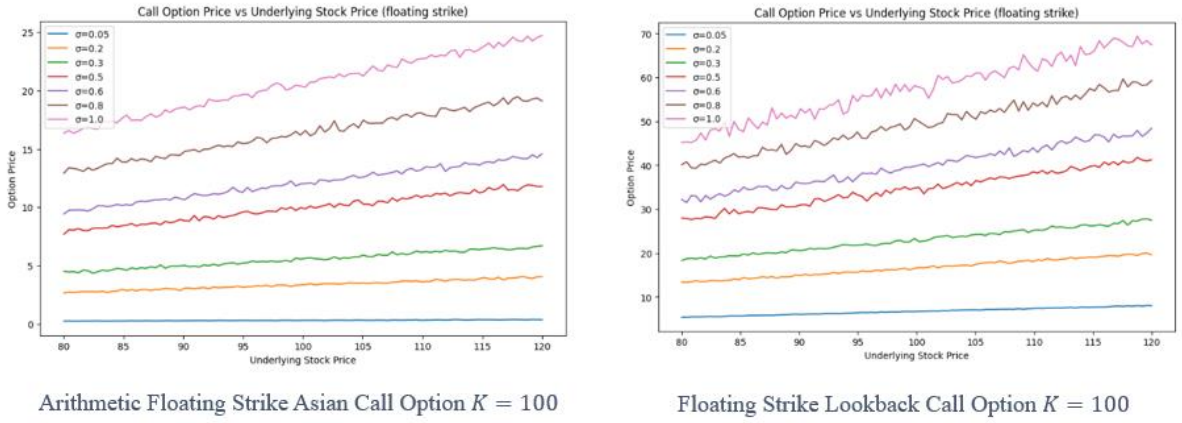

Arithmetic Floating Strike Asian Call Option $K = 100$ Floating Strike Lookback Call Option $K = 100$

Figure 5 – Floating Strike Call Option prices vs. Spot Prices

The analysis of call option prices for floating strike Lookback options across various volatility profiles reveals a pronounced dependence on volatility. Higher volatility levels significantly elevate option prices as expected and discussed in section 5.2. In contrast, lower volatility scenarios show notably stable and lower option prices, indicating a reduced potential for the asset to exceed initially observed values significantly. This behavior illustrates that floating strike Lookback options derive their value primarily from the capacity to adapt the strike price to the asset's highest or lowest observed price, thereby maximizing the payoff in environments where price fluctuations are substantial.

In addition, floating strike Lookback options exhibit a diminished sensitivity to immediate underlying price changes, as evidenced by the smooth progression of option prices, particularly under lower to moderate volatility conditions. It is shown in Figure 5. This unique characteristic highlights the

continuous recalibration of the strike price, ensuring it always aligns with the most favorable historical price. Unlike fixed strike options, which show marked shifts in valuation near specific strike zones, floating strikes maintain a more consistent valuation pattern, devoid of abrupt price changes regardless of market fluctuations. This adaptive feature of floating strike options makes them especially valuable in volatile markets, providing investors with a strategic tool for capitalizing on optimal prices throughout the life of the option.

Similar patterns can be found in floating strike Asian options.

5.6. Error Analysis of Monte Carlo Simulations

As mentioned in section 2.3, the accuracy of the Monte Carlo estimate improves with increasing the number of paths due to the law of large numbers. The standard error of the estimate can be assessed as:

$$\epsilon = \frac{\hat{\sigma}}{\sqrt{M}}$$

$\hat{\sigma}^2$ is the sample variance of $e^{-rT}S_T^{(i)}$ across M different paths. Table 2 represents the standard error estimation from Asian Option pricing across different configurations between 1000 simulation paths and 10,000 simulation paths.

Asian Option Monte Carlo Pricing Standard Error			1,000 paths	10,000 paths
Strike Type	**Option Type**	**Averaging**	**Standard Error**	**Standard Error**
Fixed	Call	Arithmetic	0.248	0.079
	Call	Geometric	0.258	0.079
	Put	Arithmetic	0.164	0.053
	Put	Geometric	0.172	0.053
Floating	Call	Arithmetic	0.170	0.053
	Call	Geometric	0.180	0.054
	Put	Arithmetic	0.266	0.079
	Put	Geometric	0.233	0.076

Table 2 – Asian Options Monte Carlo Pricing Standard Error

The results in **Table 2** from Monte Carlo simulations for pricing Asian options demonstrate the impact of increasing the number of simulation paths on the precision and stability of option pricing. Notably, when the number of paths increases from 1,000 to 10,000, there is a significant reduction in the standard error across all option types and configurations, as indicated in the table. For instance, the standard error for an Asian call option with fixed strike and arithmetic averaging decreases from 0.248 to 0.079 when the path count increases. This reduction is consistent across both fixed and floating strikes and for both arithmetic and geometric averaging methods. The effect is a clearer indication of convergence towards

a more accurate estimate of the option prices, as the law of large numbers suggests that increasing the number of trials should reduce the variability of the estimate.

Further analysis of the stability of option prices across multiple runs, as illustrated in the set in **Figure 6**, corroborates these findings. With 10,000 paths, the option prices across different runs exhibit markedly less variance compared to those from simulations with only 1,000 paths, regardless of the underlying volatility setting. This pattern holds true for both call and put options and across varying levels of volatility. The graphs distinctly presents that higher path counts not only stabilize the mean estimate of the price but also tighten the distribution of the price outcomes around this mean. This enhanced stability is crucial for accurate pricing, signifying the importance of employing a sufficient number of simulation paths in the Monte Carlo method to achieve reliable and robust results.

6. Extension I: Analytical Solutions of Pricing Asian and Lookback Options

6.1. Analytical Solutions for Pricing Asian Options

This section seeks to derive the analytical solution for pricing geometric averaging Asian options. The calculation results will be compared with the outcomes obtained from Monte Carlo simulations to evaluate the performance of this numerical scheme. Arithmetic averaging Asian options will not be further discussed here because literature and academic research demonstrate that it is not possible to find a closed-form solution (Haug 2007, Kwok 2008, Wilmott 2007 et all). Haug (2007) explains that the main reason for this observation is the non-lognormal distribution of the arithmetic average prices when the asset is assumed to follow a lognormal distribution.

Recall the risk neutral probability measure $\mathbb{Q}$ defined in section 2.1. Under $\mathbb{Q}$ measure, the discounted asset prices are martingales, implying the absence of arbitrage. Under this method, the below SDE was obtained (details can be viewed in section 2.1 and **Appendix A**):

$$\frac{dS_t}{S_t} = rdt + \sigma dW_t^{\mathbb{Q}}$$

Based on its solution (see section 2.1, 2.2), for $0 < t < T$, the solution can be written as:

$$\ln S_u = \ln S_t + \left(r - \frac{1}{2}\sigma^2\right)(u - t) + \sigma\left(W_u^{\mathbb{Q}} - W_t^{\mathbb{Q}}\right)$$

According to section 3.1, the geometric averaging method was defined as $A_t = \exp\left\{\frac{1}{t}\int_0^t \ln S_u \, du\right\}$, taking the logarithm of both sides and substituting $\ln S_u$ into A_t:

$$\ln A_t = \ln \exp\left\{\frac{1}{t}\int_0^t \ln S_u \, du\right\} = \frac{1}{t}\int_0^t \ln S_u \, du$$

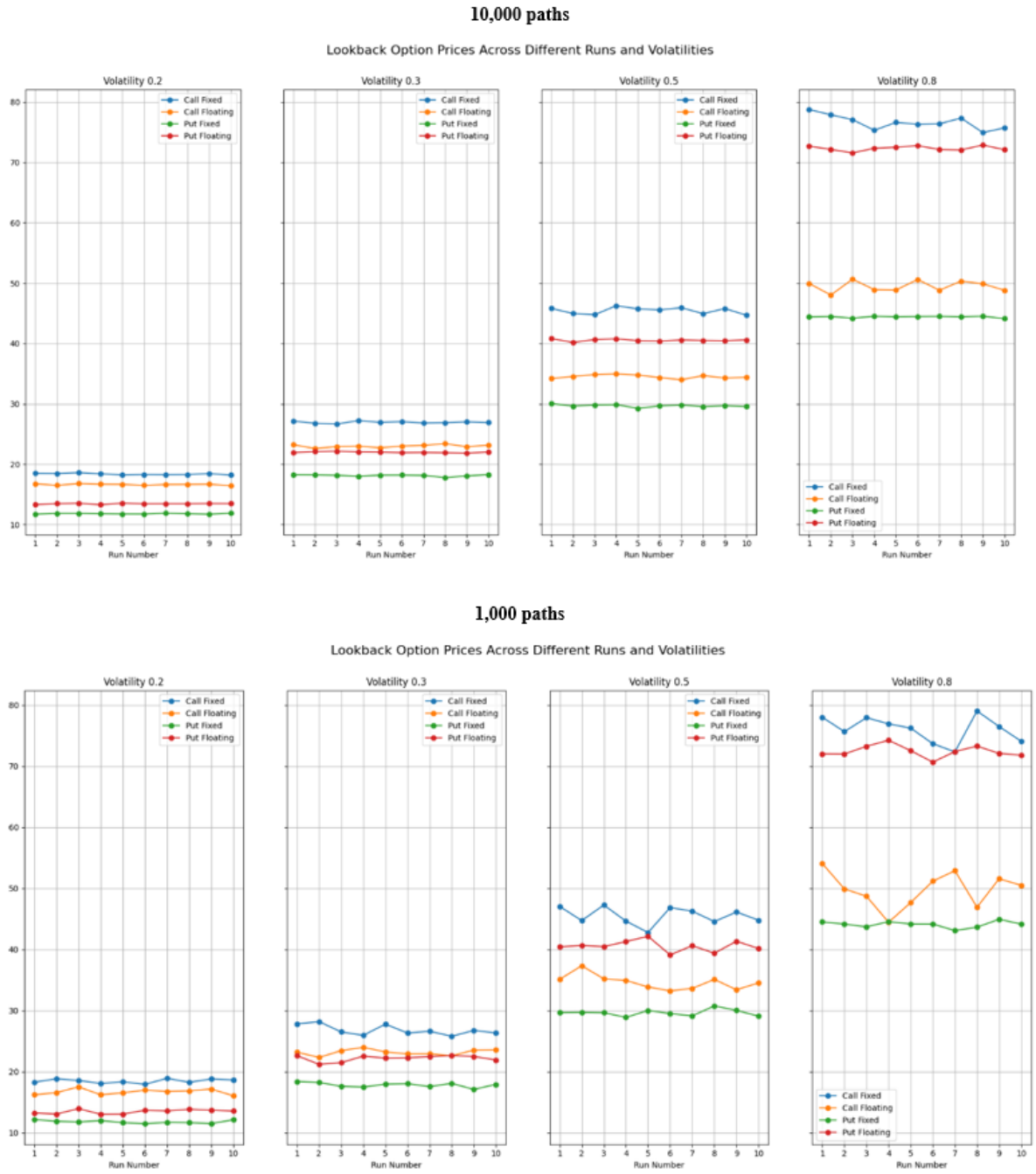

Figure 6 – Stability of Option Prices across Multiple Run

$$= \frac{1}{t}\int_0^t \left(\ln S_t + \left(r - \frac{1}{2}\sigma^2\right)(u-t) + \sigma\left(W_u^{\mathbb{Q}} - W_t^{\mathbb{Q}}\right)\right) du$$

$$= \frac{1}{t}\left(\int_0^t \ln S_t \, du + \int_0^t \left(r - \frac{1}{2}\sigma^2\right)(u-t) du + \int_0^t \sigma\left(W_u^{\mathbb{Q}} - W_t^{\mathbb{Q}}\right) du\right)$$

The first integral is easy to evaluate:

$$\int_0^t \ln S_t \, du = (t-0)\ln S_t$$

The second integral can be evaluated in the below manner since $r - \frac{1}{2}\sigma^2$ is just a constant term:

$$\int_0^t \left(r - \frac{1}{2}\sigma^2\right)(u-t) du = \left(r - \frac{1}{2}\sigma^2\right)\int_0^t (u-t) du$$

$$= \left(r - \frac{1}{2}\sigma^2\right)\left(\int_0^t u du - \int_0^t t du\right)$$

$$= \left(r - \frac{1}{2}\sigma^2\right)\left(\left[\frac{1}{2}u^2\right]_0^t - t[u]_0^t\right)$$

$$= \left(r - \frac{1}{2}\sigma^2\right)\left(\frac{1}{2}(t-0)^2 - (t-0)^2\right)$$

$$= -\frac{(t-0)^2}{2}\left(r - \frac{1}{2}\sigma^2\right)$$

Substituting the results back into $\ln A_t$:

$$\ln A_t = \frac{1}{t}\int_0^t \ln S_u \, du = \frac{1}{t}\left((t-0)\ln S_t - \frac{(t-0)^2}{2}\left(r - \frac{1}{2}\sigma^2\right) + \sigma\int_0^t \left(W_u^{\mathbb{Q}} - W_t^{\mathbb{Q}}\right) du\right)$$

Now, the focus will be shifted to expiration date T. To find $\ln A_T$, the above derivation of $\ln A_t$ can be used:

$$\ln A_T = \frac{1}{T}\int_0^T \ln S_u \, du = \frac{1}{T}\left(\int_0^t \ln S_u \, du + \int_t^T \ln S_u \, du\right)$$

$$= \frac{1}{T}\int_0^t \ln S_u \, du + \frac{1}{T}\int_t^T \ln S_u \, du$$

$$= \frac{t}{T}\left(\frac{1}{t}\int_0^t \ln S_u \, du\right) + \frac{1}{T}\int_t^T \ln S_u \, du$$

$$= \frac{t}{T}\ln A_t + \frac{1}{T}\int_t^T \ln S_u \, du$$

For the integral $\frac{1}{T}\int_t^T \ln S_u \, du$, it can be evaluated the same process as how the $\int_0^t \ln S_u \, du$ was evaluated above. The only change is the integration limits changed from $[0, t]$ to $[t, T]$. As a result, the below equation can be obtained:

$$\ln A_T = \frac{t}{T}\ln A_t + \frac{1}{T}\left[(T-t)\ln S_t + \left(r - \frac{1}{2}\sigma^2\right)\frac{(T-t)^2}{2}\right] + \frac{\sigma}{T}\int_t^T \left(W_u^{\mathbb{Q}} - W_t^{\mathbb{Q}}\right)du$$

Now, let's focus on the stochastic term $\frac{\sigma}{T}\int_t^T \left(W_u^{\mathbb{Q}} - W_t^{\mathbb{Q}}\right)du$, it can be shown to be Gaussian with zero mean and a variance. This is because the Brownian motion increments $W_u^{\mathbb{Q}} - W_t^{\mathbb{Q}}$ from time u to t is normally distributed with mean 0 and variance $u - t$.

$$W_u^{\mathbb{Q}} - W_t^{\mathbb{Q}} \sim \mathcal{N}(0, u-t)$$

The integral of the variance of the Brownian increment can be expressed as the squared integral below:

$$\left(\int_t^T \left(W_u^{\mathbb{Q}} - W_t^{\mathbb{Q}}\right)du\right)^2$$

Given the covariance of $W_u^{\mathbb{Q}} - W_t^{\mathbb{Q}}$ and $W_v^{\mathbb{Q}} - W_t^{\mathbb{Q}}$ for $u, v \geq t$ is $\min(u, v) - t$ (the proof can be seen in **Appendix E**), thus, the expectation of the squared integral becomes:

$$\mathbb{E}\left[\left(\int_t^T \left(W_u^{\mathbb{Q}} - W_t^{\mathbb{Q}}\right)du\right)^2\right] = \int_t^T \int_t^T (\min(u, v) - t)\, dudv$$

Breaking into two parts (where $u < v$ and $u \geq v$):

$$\min(u, v) = \begin{cases} u, & u < v \\ v, & u \geq v \end{cases}$$

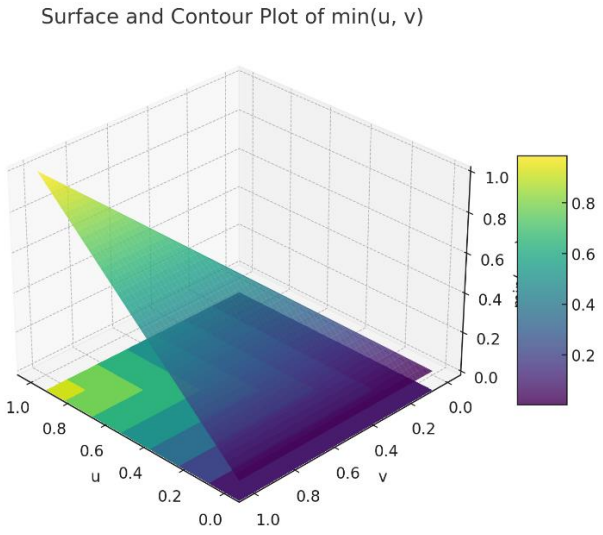

Figure 7 – Surface and Contour Plot of min(u,v)

The integral of the $\min(u, v)$ function over the square $[t, T] \times [t, T]$ is symmetrical about the line $u = v$, which divides the square into two equal triangles. One triangle where $u < v$, the other where $u \geq v$. For each specific point (u, v) in the triangle where $u < v$, there is a corresponding point (v, u) in the triangle $u \geq v$. At these points, the value of $\min(u, v)$ is the same. Therefore, the integration of $\min(u, v) - t$ over the region where $u < v$ will yield the same result as over the region where $u \geq v$ because of this symmetric relationship. This is visualized for $t = 0, T = 1$ in the below figure:

This plot displays both a surface and contour view of the function across the u, v plane. The surface plot shows how the value of $\min(u, v)$ changes based on the coordinates u and v. As can be seen in the figure, the function takes the value of whichever variable is smaller, creating a linear gradient in two directions on the surface. Below the surface, the contour plot on the u, v plane illustrates lines of equal value. The line $u = v$, which runs from the bottom left to the top right of the plane, effectively divides the space into two symmetric regions. On the side above this line, $\min(u, v) = v$, on the side below this line, $\min(u, v) = u$.

This symmetry relationship allows us to compute the integral over one half of the domain and then double it to get the full integral. Therefore, the double integral can be simplified as (considering $u < v$):

$$\int_t^T \int_t^T (\min(u, v) - t)\, dudv = 2 \int_t^T \int_t^T (u - t)\, dudv$$

Compute the inner integral du first:

$$2 \int_t^T \int_t^T (u - t)\, dudv = 2 \int_t^T \left(\int_t^v (u - t) du \right) dv = 2 \int_t^T \left(\left[\frac{u^2}{2} - ut \right]_t^v \right) dv$$

$$= 2 \int_t^T \left(\frac{v^2}{2} - vt - \frac{t^2}{2} + t^2 \right) dv = 2 \int_t^T \left(\frac{v^2}{2} - vt + \frac{t^2}{2} \right) dv$$

Simplify the component inside the integral:

$$\frac{v^2}{2} - vt + \frac{t^2}{2} = \frac{v^2 - 2vt + t^2}{2} = \frac{(v - t)^2}{2}$$

Substituting this back to the integral, and the outer integral dv can be computed:

$$2 \int_t^T \left(\frac{v^2}{2} - vt + \frac{t^2}{2} \right) dv = 2 \int_t^T \left(\frac{(v - t)^2}{2} \right) dv = \int_t^T (v - t)^2 dv$$

Change of variable: $s = v - t$, $\frac{ds}{dv} = 1$, thus, the limits of the integral change into $[0, T - t]$:

$$\int_0^{T-t} s^2\, ds = \left[\frac{s^3}{3} \right]_0^{T-t} = \frac{(T - t)^3}{3}$$

As a result, the expectation of the squared integral is:

$$\mathbb{E}\left[\left(\int_t^T (W_u^{\mathbb{Q}} - W_t^{\mathbb{Q}})du\right)^2\right] = \frac{(T-t)^3}{3}$$

Recall the stochastic term $\frac{\sigma}{T}\int_t^T (W_u^{\mathbb{Q}} - W_t^{\mathbb{Q}})du$, the normalized variance is:

$$\left(\frac{\sigma}{T}\right)^2 \frac{(T-t)^3}{3} = \frac{\sigma^2(T-t)^3}{3T^2}$$

Therefore, the distribution for the stochastic term is

$$\frac{\sigma}{T}\int_t^T (W_u^{\mathbb{Q}} - W_t^{\mathbb{Q}})du \sim \mathcal{N}\left(0, \frac{\sigma^2(T-t)^3}{3T^2}\right)$$

Based on the risk neutral principle and recall the payoff definition of European fixed strike Asian call option:

$$C_{fixed}(S,t) = e^{-r(T-t)}\mathbb{E}^{\mathbb{Q}}[\max(A_T - K, 0)]$$

Note that the expectation is taken under $\mathbb{Q}$ conditional on the filtration generated by the $\mathbb{Q}$-Brownian motion. Now, given the distribution of the stochastic term, let's write the $\ln A_T$ process with respect to a newly defined standard normal variable $\tilde{Z}$:

$$\tilde{Z} = \frac{\int_t^T (Z_u^{\mathbb{Q}} - Z_t^{\mathbb{Q}})du}{\sqrt{\frac{(T-t)^3}{3}}}$$

$$\frac{\sigma}{T}\int_t^T (W_u^{\mathbb{Q}} - W_t^{\mathbb{Q}})du = \frac{\sigma}{T}\sqrt{\frac{(T-t)^3}{3}}\frac{\int_t^T (Z_u^{\mathbb{Q}} - Z_t^{\mathbb{Q}})du}{\sqrt{\frac{(T-t)^3}{3}}} = \frac{\sigma}{T}\sqrt{\frac{(T-t)^3}{3}}\tilde{Z}$$

Define the new drift and diffusion under new measure $\tilde{Z}$, which follows a standard Brownian motion:

$$\tilde{\mu} = \left(r - \frac{1}{2}\sigma^2\right)\frac{(T-t)^2}{2T}$$

$$\tilde{\sigma} = \frac{\sigma}{T}\sqrt{\frac{(T-t)^3}{3}}$$

Therefore, $\ln A_T$ becomes:

$$\ln A_T = \frac{t}{T}\ln A_t + \frac{1}{T}(T-t)\ln S_t + \tilde{\mu} + \tilde{\sigma}\tilde{Z}$$

Taking exponentials on both sides, and define a new variable $F_t = A_t^{\frac{t}{T}} S_t^{\frac{(T-t)}{T}}$ the equation becomes:

$$A_T = A_t^{\frac{t}{T}} S_t^{\frac{(T-t)}{T}} e^{\tilde{\mu}+\tilde{\sigma}\tilde{Z}} = F_t e^{\tilde{\mu}+\tilde{\sigma}\tilde{Z}}$$

Looking back to the European fixed strike Asian call option payoff:

$$\mathbb{E}^{\mathbb{Q}}[\max(A_T - K, 0)] = \mathbb{E}^{\mathbb{Q}}\left[\max\left(F_t e^{\tilde{\mu}+\tilde{\sigma}\tilde{Z}} - K, 0\right)\right]$$

Define an indicator function $\mathbb{I}_{\{A\}}$ such that:

$$\mathbb{I}_{\{A\}} = \mathbb{E}^{\mathbb{Q}}\left[\mathbb{I}_{\{A\}}\right] = \int_{\Omega} \mathbb{I}_{\{A\}}\, d\mathbb{Q} = \int_{A} 1\, d\mathbb{Q} + \int_{\Omega - A} 0\, d\mathbb{Q} = \mathbb{Q}\{A\}$$

Thus, substitute this concept into the payoff function, and let's divide it into 2 components:

$$\mathbb{E}^{\mathbb{Q}}\left[\max\left(F_t e^{\tilde{\mu}+\tilde{\sigma}\tilde{Z}} - K, 0\right)\right] = \underbrace{\mathbb{E}^{\mathbb{Q}}\left[F_t e^{\tilde{\mu}+\tilde{\sigma}\tilde{Z}} \mathbb{I}_{\{A_T > K\}}\right]}_{1} - \underbrace{\mathbb{E}^{\mathbb{Q}}\left[K\, \mathbb{I}_{\{A_T > K\}}\right]}_{2}$$

Start with component 2:

$$\mathbb{E}^{\mathbb{Q}}\left[K\, \mathbb{I}_{\{A_T > K\}}\right] = K\mathbb{E}^{\mathbb{Q}}\left[\mathbb{I}_{\{A_T > K\}}\right] = K\, \Pr_{\mathbb{Q}}\{A_T > K\} = K\, \Pr_{\mathbb{Q}}\left\{F_t e^{\tilde{\mu}+\tilde{\sigma}\tilde{Z}} > K\right\}$$

$$= K\, \Pr_{\mathbb{Q}}\left\{\frac{F_t e^{\tilde{\mu}+\tilde{\sigma}\tilde{Z}}}{K} > 1\right\} = K\, \Pr_{\mathbb{Q}}\left\{\ln\left(\frac{F_t}{K}\right) + \tilde{\mu} + \tilde{\sigma}\tilde{Z} > 0\right\}$$

$$= K\, \Pr_{\mathbb{Q}}\left\{\ln\left(\frac{F_t}{K}\right) + \tilde{\mu} > -\tilde{\sigma}\tilde{Z}\right\}$$

Knowing that $\tilde{Z}$ is a standard normal random variable, and due to the symmetric property of normal distribution:

$$K\, \Pr_{\mathbb{Q}}\left\{\ln\left(\frac{F_t}{K}\right) + \tilde{\mu} > -\tilde{\sigma}\tilde{Z}\right\} = K\, \Pr_{\mathbb{Q}}\left\{\frac{\ln\left(\frac{F_t}{K}\right) + \tilde{\mu}}{\tilde{\sigma}} > \tilde{Z}\right\} = KN\left(\frac{\ln\left(\frac{F_t}{K}\right) + \tilde{\mu}}{\tilde{\sigma}}\right)$$

Let's look back at component 1, and extend it into integration form:

$$\mathbb{E}^{\mathbb{Q}}\left[F_t e^{\tilde{\mu}+\tilde{\sigma}\tilde{Z}} \mathbb{I}_{\{A_T > K\}}\right] = \int_{\Omega} F_t e^{\tilde{\mu}+\tilde{\sigma}\tilde{Z}}\, \mathbb{I}_{\{A_T > K\}}\, d\mathbb{Q}$$

To further solve this integration, change of measure needs to be applied, thus, Girsanov Theorem. It is necessary to define a martingale process to satisfy the below Radon Nikodym derivative $\tilde{\Lambda}$ with the newly defined measure $\tilde{\mathbb{Q}}$:

$$\frac{d\widetilde{\mathbb{Q}}}{d\mathbb{Q}} = \widetilde{\Lambda} = e^{\tilde{\sigma}W_T^{\mathbb{Q}} - \frac{1}{2}\tilde{\sigma}^2 T}$$

Therefore, substitute it back into the integral:

$$\int_\Omega F_t e^{\tilde{\mu}+\tilde{\sigma}\tilde{Z}}\, \mathbb{I}_{\{A_T>K\}}\, d\mathbb{Q} = \int_\Omega F_t e^{\tilde{\mu}+\tilde{\sigma}\tilde{Z}}\, e^{\tilde{\sigma}W_T^{\mathbb{Q}} - \frac{1}{2}\tilde{\sigma}^2 T}\, \mathbb{I}_{\{A_T>K\}}\, d\mathbb{Q}$$

$$= \int_\Omega F_t e^{\tilde{\mu}+\frac{1}{2}\tilde{\sigma}^2}\, e^{\tilde{\sigma}^2}\, e^{\tilde{\sigma}W_T^{\mathbb{Q}} - \frac{1}{2}\,\tilde{\sigma}^2 T}\, \mathbb{I}_{\{A_T>K\}}\, d\mathbb{Q} = F_t e^{\tilde{\mu}+\frac{1}{2}\tilde{\sigma}^2} \int_\Omega \frac{d\widetilde{\mathbb{Q}}}{d\mathbb{Q}}\, \mathbb{I}_{\{A_T>K\}}\, d\mathbb{Q}$$

$$= F_t e^{\tilde{\mu}+\frac{1}{2}\tilde{\sigma}^2} \int_\Omega \mathbb{I}_{\{A_T>K\}}\, d\widetilde{\mathbb{Q}} = F_t e^{\tilde{\mu}+\frac{1}{2}\tilde{\sigma}^2} \Pr_{\widetilde{\mathbb{Q}}}\left\{F_t e^{\tilde{\mu}+\tilde{\sigma}^2+\tilde{\sigma}W_T^{\widetilde{\mathbb{Q}}}} > K\right\}$$

$$= F_t e^{\tilde{\mu}+\frac{1}{2}\tilde{\sigma}^2} \Pr_{\widetilde{\mathbb{Q}}}\left\{\ln\left(\frac{F_t}{K}\right) + \tilde{\mu} + \tilde{\sigma}^2 > -\tilde{\sigma}W_T^{\widetilde{\mathbb{Q}}}\right\}$$

$$= F_t e^{\tilde{\mu}+\frac{1}{2}\tilde{\sigma}^2} \Pr_{\widetilde{\mathbb{Q}}}\left\{\frac{\ln\left(\frac{F_t}{K}\right) + \tilde{\mu} + \tilde{\sigma}^2}{\tilde{\sigma}} > W_T^{\widetilde{\mathbb{Q}}}\right\} = F_t e^{\tilde{\mu}+\frac{1}{2}\tilde{\sigma}^2} N\left(\frac{\ln\left(\frac{F_t}{K}\right) + \tilde{\mu} + \tilde{\sigma}^2}{\tilde{\sigma}}\right)$$

As a result, the payoff for European fixed strike Asian call option can be written as:

$$C_{fixed}(S,t) = e^{-r(T-t)}\mathbb{E}^{\mathbb{Q}}[\max(A_T - K, 0)]$$

$$= e^{-r(T-t)}\left[F_t e^{\tilde{\mu}+\frac{1}{2}\tilde{\sigma}^2} N\left(\frac{\ln\left(\frac{F_t}{K} + \tilde{\mu} + \tilde{\sigma}^2\right)}{\tilde{\sigma}}\right) - KN\left(\frac{\ln\left(\frac{F_t}{K}\right) + \tilde{\mu}}{\tilde{\sigma}}\right)\right]$$

$$= e^{-r(T-t)}\left[A_t^{\frac{t}{T}} S_t^{\frac{(T-t)}{T}} e^{\tilde{\mu}+\frac{1}{2}\tilde{\sigma}^2} N(d_1) - KN(d_2)\right]$$

$$d_2 = \frac{\ln\left(\frac{F_t}{K}\right) + \tilde{\mu}}{\tilde{\sigma}} = \frac{\frac{t}{T}\ln A_t + \frac{1}{T}(T-t)\ln S_t + \left(r - \frac{1}{2}\sigma^2\right)\frac{(T-t)^2}{2T} - \ln K}{\frac{\sigma}{T}\sqrt{\frac{(T-t)^3}{3}}}$$

$$d_1 = \frac{\ln\left(\frac{F_t}{K} + \tilde{\mu} + \tilde{\sigma}^2\right)}{\tilde{\sigma}} = \frac{\frac{t}{T}\ln A_t + \frac{1}{T}(T-t)\ln S_t + \left(r - \frac{1}{2}\sigma^2\right)\frac{(T-t)^2}{2T} - \ln K + \left(\frac{\sigma}{T}\right)^2\frac{(T-t)^3}{3}}{\frac{\sigma}{T}\sqrt{\frac{(T-t)^3}{3}}}$$

$$= d_2 + \tilde{\sigma}$$

The corresponding call option pricing formula will be shown below with the same d_1, d_2 above:

$$P_{fixed} = \max(K - A_T, 0) = e^{-r(T-t)}\left[KN(d_2) - A_t^{\frac{t}{T}} S_t^{\frac{(T-t)}{T}} e^{\tilde{\mu}+\frac{1}{2}\tilde{\sigma}^2} N(d_1)\right]$$

These analytical results align with what Wilmott (2007) presents in the book.

Next, let's consider the floating strike Asian option. The terminal payoff of the floating strike Asian call option involves both S_T and A_T, joint distribution of S_T and A_T will be required to price this type of option under risk neutral probability measure. Denote the value of the option as $C_{floating}(S, I, t)$. The differential equation for all $0 < t < T$ is constructed as below.

Prior to expiry we have information about the possible final value of S at time T in the present value of S at time t. or example, the higher S is today, the higher it will probably end up at expiry. Similarly, we have information about the possible final value of I in the value of the integral to date $I(t)$. As we get closer to expiry, we become more confident about the final value of I. Therefore, one can imagine that the value of the option is therefore not only a function of S and t, but also a function of I (Ahmad Riaz 2024 Lecture 5 – Exotic Options, CQF 2024 Jan Cohort). I will be the new independent variable called state variable. In this problem set, the state variable is:

$$I(t) = \int_0^t f(S, \tau)\, d\tau = \int_0^t \ln S_\tau \, d\tau$$

The value of the contract is now a function of the three variables $C(S, I, t)$. Due to arbitrage free, we set up a portfolio containing one of the path-dependent option and short a number Δ of the underlying asset (this is a delta-hedged portfolio, not the self-financing portfolio):

$$\Pi = C(S, I, t) - \Delta S$$

The change in value of this portfolio is given by: (Derived from $d\Pi = d(C - \Delta S)$):

$$d\Pi = \left(\frac{\partial C}{\partial t} + \frac{1}{2}\sigma^2 S^2 \frac{\partial^2 C}{\partial S^2}\right) dt + \frac{\partial C}{\partial I} dI + \left(\frac{\partial C}{\partial S} - \Delta\right) dS$$

Now, we choose $\Delta = \frac{\partial C}{\partial S}$ to eliminate risk → Risk neutral → As a result:

$$d\Pi = \left(\frac{\partial C}{\partial t} + \frac{1}{2}\sigma^2 S^2 \frac{\partial^2 C}{\partial S^2}\right) dt + \frac{\partial C}{\partial I} dI = \left(\frac{\partial C}{\partial t} + \frac{1}{2}\sigma^2 S^2 \frac{\partial^2 C}{\partial S^2} + f(S, t)\frac{\partial C}{\partial I}\right) dt$$

Note that $d\Pi$ becomes risk free, and thus, earns the risk free rate of the interest r, therefore:

$$d\Pi = r\Pi dt = r(C - \Delta S)dt = r\left(C - \frac{\partial C}{\partial S} S\right) dt$$

This is leading to the non-arbitrage pricing equation:

$$r\left(C - \frac{\partial C}{\partial S} S\right) dt = \left(\frac{\partial C}{\partial t} + \frac{1}{2}\sigma^2 S^2 \frac{\partial^2 C}{\partial S^2} + f(S, t)\frac{\partial C}{\partial I}\right) dt$$

This is to be solved subject to $C(S,I,T) = u_i(S,I)$, where u_i denotes payoff. This completes the formulation of the valuation problem.

$$\frac{\partial C}{\partial t} + \frac{1}{2}\sigma^2 S^2 \frac{\partial^2 C}{\partial S^2} + f(S,t)\frac{\partial C}{\partial I} + rS\frac{\partial C}{\partial S} - rC = 0$$

As a result:

$$\frac{\partial C_{floating}}{\partial t} + \frac{1}{2}\sigma^2 S^2 \frac{\partial^2 C_{floating}}{\partial S^2} + \frac{A}{t}\ln\frac{S}{A}\frac{\partial C_{floating}}{\partial A} + rS\frac{\partial C_{floating}}{\partial S} - rC_{floating} = 0$$

To further process, similarity reduction can be applied here. Recall the payoff of the European floating strike Asian call option: $\max(S_T - A_T, 0)$. By taking out the component of S_T, the terminal payoff becomes $\frac{1}{S_T}\max\left(1 - \frac{A_T}{S_T}, 0\right)$. Define similarity variables:

$$R = t\ln\frac{A}{S}; W(R,t) = \frac{C_{floating}}{S}$$

So that the value of the option becomes $C_{floating} = SW(R,t)$. Finding the relevant partial derivatives:

$$\frac{\partial R}{\partial t} = \ln\frac{A}{S}; \frac{\partial R}{\partial S} = \frac{\partial}{\partial S}\left(t\ln\frac{A}{S}\right) = \frac{\partial}{\partial S}\left(t(\ln A - \ln S)\right) = \left(t\left(0 - \frac{1}{S}\right)\right) = -\frac{t}{S}$$

$$\frac{\partial R}{\partial A} = \frac{\partial}{\partial A}\left(t(\ln A - \ln S)\right) = \frac{t}{A}$$

Applying the chain rule here:

$$\frac{\partial C_{floating}}{\partial t} = S\frac{\partial W}{\partial t} + W\frac{\partial S}{\partial t}$$

Using the chain rule:

$$\frac{\partial W}{\partial t} = \frac{\partial W}{\partial R}\frac{\partial R}{\partial t} + \frac{\partial W}{\partial t} = \frac{\partial W}{\partial R}\ln\frac{A}{S} + \alpha\frac{\partial W}{\partial t}$$

Additional information is needed to find $\frac{\partial W}{\partial t}$.

$$\frac{\partial C_{floating}}{\partial S} = W + S\frac{\partial W}{\partial S} = W + S\frac{\partial W}{\partial R}\frac{\partial R}{\partial S} = W - t\frac{\partial W}{\partial R}$$

$$\frac{\partial^2 C_{floating}}{\partial S^2} = \frac{\partial}{\partial S}\left(W + S\frac{\partial W}{\partial S}\right) = 2\frac{\partial W}{\partial S} + S\frac{\partial^2 W}{\partial S^2} = 2\frac{\partial W}{\partial S} + S\left(\frac{\partial}{\partial S}\left(\frac{\partial W}{\partial R}\frac{\partial R}{\partial S}\right)\right)$$

$$= \frac{\partial W}{\partial R}\frac{\partial^2 R}{\partial S^2} + \frac{\partial^2 W}{\partial R^2}\left(\frac{\partial R}{\partial S}\right)^2 = \frac{t}{S^2}\frac{\partial W}{\partial R} + \frac{\partial^2 W}{\partial R^2}\left(\frac{\partial R}{\partial S}\right)^2$$

Subsisting everything into the original differential equation. The result is unfortunately not the desired type of differential equation. Based on Kwok (2008) and Haug (2007), the ultimately differential equation should be something that can be easily reducible to one dimensional heat equation.

Additionally, the trial of Asian option analytical solutions does not seem to be successful, the pricing result from fixed strike geometric Asian call option also does not seem to be correct. It is possible that one of the final condition was missing, and the change of measure process might have gone wrong, since the geometric average has to larger than the fixed strike price to enable option to have payoffs. More time will be needed to further investigate.

6.2. Analytical Solutions for Pricing Lookback Options

The specific calculations for $\mathbb{E}^{\mathbb{Q}}\left[S_T - \min_{0\le t\le T} S_t\right]$ involves integral solutions or approximations based on the joint distribution of S_T and $m_0^T = \min_{0\le t\le T} S_t$. Kwok (2008) suggests that it is also possible to adopt the usual Black-Scholes pricing framework to derive the analytical solution for lookback options pricing. Initiated by Kwok (2008) and Haug (2007), define a stochastic variable $U_\xi = \ln\frac{S_\xi}{S}$, and it is a Brownian motion with drift $r - \frac{1}{2}\sigma^2$ and variance σ^2. Recall the definition of $m_0^T = \min_{0\le t\le T} S_t$ and $M_0^T = \max_{0\le t\le T} S_t$ in section 3.2, let's define new stochastic variables based on this:

$$y_T = \ln\frac{m_0^T}{S} = \min\{U_\xi, \xi \in [0,T]\}$$

$$Y_T = \ln\frac{M_0^T}{S} = \max\{U_\xi, \xi \in [0,T]\}$$

The joint distribution function of U_T and y_T can be deduced from the transition density function of the Brownian motion process. To start with, to find the probability $\Pr\{U_T > u, Y_T < y\}$, define a random process

$$\widetilde{U_t} = \begin{cases} U_t, & t < \xi \\ 2y - U_t, & \xi \le t \le T \end{cases}$$

$\widetilde{U_t}$ is a mirror reflection of U_t at the level y within the time interval $\xi \le t \le T$, thus the spaces $\{U_T > u\}$ and $\{\widetilde{U_t} < 2y - u\}$ are equivalent given any $0 \le u \le U_t$. Therefore, the below relation can be derived:

$$\Pr\{U_T > u, y_T < y\} = \Pr\{\widetilde{U_T} < 2y - u\} = \Pr\{U_T < 2y - u\} = N\left(\frac{2y-u}{\sigma\sqrt{T}}\right)$$

Moreover, Girsanov Theorem can be applied to effect the change of measure because Brownian motion has nonzero drift in this case. Define probability measure $\mathbb{Q}$ such that U_t^μ is a stochastic process with drift μ, now a new measure $\widetilde{\mathbb{Q}}$ is needed to transform U_t^μ to a process without drift.

Consider the joint distribution:

$$\Pr\{U_T > u, y_T < y\} = \mathbb{E}^{\mathbb{Q}}\left[\mathbb{I}_{\{U_T^\mu > u\}} \times \mathbb{I}_{\{Y_T < y\}}\right] = \mathbb{E}^{\widetilde{\mathbb{Q}}}\left[\mathbb{I}_{\{U_T^\mu > u\}} \times \mathbb{I}_{\{Y_T < y\}} \exp\left\{\frac{\mu U_T^\mu}{\sigma^2} - \frac{\mu^2 T}{2\sigma^2}\right\}\right]$$

$$= \mathbb{E}^{\widetilde{\mathbb{Q}}}\left[\mathbb{I}_{\{2y - U_T^\mu > u\}} \exp\left\{\frac{\mu\left(2y - U_T^\mu\right)}{\sigma^2} - \frac{\mu^2 T}{2\sigma^2}\right\}\right]$$

$$= e^{\frac{2\mu y}{\sigma^2}} \mathbb{E}^{\widetilde{\mathbb{Q}}}\left[\mathbb{I}_{\{U_T^\mu < 2y - u\}} \exp\left\{\frac{\mu}{\sigma^2} U_T^\mu - \frac{\mu^2 T}{2\sigma^2}\right\}\right]$$

$$= e^{\frac{2\mu y}{\sigma^2}} \int_{-\infty}^{2y-u} \frac{1}{\sqrt{2\pi\sigma^2 T}} e^{-\frac{z^2}{2\sigma^2 T}} e^{\frac{-\mu z}{\sigma^2} - \frac{\mu^2 T}{2\sigma^2}} dz$$

$$= e^{\frac{2\mu y}{\sigma^2}} \int_{-\infty}^{2y-u} \frac{1}{\sqrt{2\pi\sigma^2 T}} e^{-\frac{(z+\mu T)^2}{2\sigma^2 T}} dz = e^{\frac{2\mu y}{\sigma^2}} N\left(\frac{2y - u + \mu T}{\sigma\sqrt{T}}\right)$$

As a result:

$$\Pr\{U_T > u, y_T > y\} = \Pr\left\{U_T^\mu > u\right\} - \Pr\left\{U_T^\mu > u, y_T < y\right\}$$

$$= N\left(\frac{-u + uT}{\sigma\sqrt{T}}\right) - e^{\frac{2\mu y}{\sigma^2}} N\left(\frac{2y - u + \mu T}{\sigma\sqrt{T}}\right)$$

Write $\tau = T - t$, and the joint distribution becomes:

$$\Pr\{U_T \geq u, y_T \geq y\} = N\left(\frac{-u + u\tau}{\sigma\sqrt{\tau}}\right) - e^{\frac{2\mu y}{\sigma^2}} N\left(\frac{2y - u + \mu\tau}{\sigma\sqrt{\tau}}\right)$$

Similarly, due to the mirroring fact between y_T and Y_T:

$$\Pr\left\{U_T^\mu < u, Y_T > y\right\} = e^{\frac{2\mu y}{\sigma^2}} N\left(\frac{2y - u - \mu\tau}{\sigma\sqrt{\tau}}\right)$$

Therefore, similarly, the below probability can be deduced:

$$\Pr\left\{U_T^\mu \leq u, Y_T \leq y\right\} = N\left(\frac{u - \mu\tau}{\sigma\sqrt{\tau}}\right) - e^{\frac{2\mu y}{\sigma^2}} N\left(\frac{2y - u - \mu\tau}{\sigma\sqrt{\tau}}\right)$$

Consider the fixed strike lookback call options,

$$C_{fixed}(S, t) = e^{-r\tau}\mathbb{E}^{\mathbb{Q}}[\max(M_0^T - K, 0)]$$

$$= e^{-r\tau} \int_0^\infty \Pr\{M_0^T - K \geq u\}\, du$$

$$= e^{-r\tau} \int_K^\infty \Pr\left\{\ln\frac{M_0^T}{S} - \ln\frac{z}{S} \geq 0\right\} dz$$

Note that the $z = u + K$ is a new variable, S can be taken out from the probability bracket:

$$= e^{-r\tau} \int_{\ln\frac{K}{S}}^{\infty} Se^{y} \Pr\{Y_T \geq y\}\, dy$$

Recall that we have defined $y = \ln\frac{m_0^T}{S}$, and $\Pr\{U_T^{\mu} \leq u, Y_T \leq y\}$ is already derived above, and by taking $y = u$, the probability of $\Pr\{Y_T \leq y\}$ can be easily obtained:

$$\Pr\{Y_T \leq y\} = N\left(\frac{y - \mu\tau}{\sigma\sqrt{\tau}}\right) - e^{\frac{2\mu y}{\sigma^2}} N\left(\frac{-y - \mu\tau}{\sigma\sqrt{\tau}}\right)$$

Therefore, by transforming $\Pr\{Y_T \leq y\}$ into $\Pr\{Y_T \geq y\}$ and substitute it back into the integration:

$$e^{-r\tau} \int_{\ln\frac{K}{S}}^{\infty} Se^{y} \Pr\{Y_T \geq y\}\, dy = e^{-r\tau} \int_{\ln\frac{K}{S}}^{\infty} Se^{y} \left[N\left(\frac{-y + \mu\tau}{\sigma\sqrt{\tau}}\right) - e^{\frac{2\mu y}{\sigma^2}} N\left(\frac{-y - \mu\tau}{\sigma\sqrt{\tau}}\right)\right] dy$$

$$= e^{-r\tau} \int_{\ln\frac{K}{S}}^{\infty} Se^{y} \left[N\left(\frac{-y + \mu\tau}{\sigma\sqrt{\tau}}\right)\right] dy - e^{-r\tau} \int_{\ln\frac{K}{S}}^{\infty} e^{\frac{2\mu y}{\sigma^2}} N\left(\frac{-y - \mu\tau}{\sigma\sqrt{\tau}}\right) dy$$

Change of variable: let $x = \frac{-y + \mu\tau}{\sigma\sqrt{\tau}}$, and rearrange: $y = -\sigma\sqrt{\tau}x + \mu\tau$, take differentials:

$$dy = -\sigma\sqrt{\tau}dx$$

Substitute it back into the first part of the integral:

$$e^{-r\tau} \int_{\ln\frac{K}{S}}^{\infty} Se^{y} \left[N\left(\frac{-y + \mu\tau}{\sigma\sqrt{\tau}}\right)\right] dy = \int_{\frac{-\ln\left(\frac{K}{S}\right) + \mu\tau}{\sigma\sqrt{\tau}}}^{\infty} Se^{-x\sigma\sqrt{\tau} + \mu\tau} N(x)\left(-\sigma\sqrt{\tau}\right) dx$$

$$= -S\sigma\sqrt{\tau}e^{\mu\tau} \int_{\frac{-\ln\left(\frac{K}{S}\right) + \mu\tau}{\sigma\sqrt{\tau}}}^{\infty} e^{-x\sigma\sqrt{\tau}} N(x) dx$$

Similar approach can be applied to the second integral:

$$e^{-r\tau} \int_{\ln\frac{K}{S}}^{\infty} e^{\frac{2\mu y}{\sigma^2}} N\left(\frac{-y - \mu\tau}{\sigma\sqrt{\tau}}\right) dy = \int_{\frac{-\ln\left(\frac{K}{S}\right) + \mu\tau}{\sigma\sqrt{\tau}}}^{\infty} e^{2\left(-x\sigma\sqrt{\tau} - \mu\tau\right)} N(x)(-\sigma\sqrt{\tau}) dx$$

$$= -\sigma\sqrt{\tau}e^{-2\mu\tau} \int_{\frac{-\ln\left(\frac{K}{S}\right) + \mu\tau}{\sigma\sqrt{\tau}}}^{\infty} e^{2x\sigma\sqrt{\tau}} N(x) dx$$

Therefore, the original integral becomes:

$$e^{-r\tau} \int_{\ln\frac{K}{S}}^{\infty} Se^{y} \left[N\left(\frac{-y + \mu\tau}{\sigma\sqrt{\tau}}\right)\right] dy - e^{-r\tau} \int_{\ln\frac{K}{S}}^{\infty} e^{\frac{2\mu y}{\sigma^2}} N\left(\frac{-y - \mu\tau}{\sigma\sqrt{\tau}}\right) dy$$

$$= -S\sigma\sqrt{\tau}e^{\mu\tau}\int_{\frac{-\ln\left(\frac{K}{S}\right)+\mu\tau}{\sigma\sqrt{\tau}}}^{\infty} e^{-x\sigma\sqrt{\tau}}N(x)dx - \sigma\sqrt{\tau}e^{-2\mu\tau}\int_{\frac{-\ln\left(\frac{K}{S}\right)+\mu\tau}{\sigma\sqrt{\tau}}}^{\infty} e^{2x\sigma\sqrt{\tau}}N(x)dx$$

By further rearranging and using the definition of normal distribution cdf, the below result can be obtained, which aligns with Haug (2007), Wilmott (2007) and Kwok (2008).

$$C_{fixed} = SN(d_1) - Ke^{-rT}N(d_2) + Se^{-rT}\frac{\sigma^2}{2r} \times \left(-\left(\frac{S}{K}\right)^{-\frac{2r}{\sigma^2}} N\left(d_1 - \frac{2r}{\sigma}\sqrt{T}\right) + e^{rT}N(d_1) \right)$$

$$d_1 = \frac{\ln\left(\frac{S}{K}\right) + \left(r + \frac{1}{2}\sigma^2\right)T}{\sigma\sqrt{T}}$$

$$d_2 = d_1 - \sigma\sqrt{T}$$

Similarly, the solution of floating strike lookback call option is priced similarly by Haug (2007):

$$C_{floating} = SN(a_1) - S_{min}e^{-rT}N(a_2) + Se^{-rT}\frac{\sigma^2}{2r} \times \left(\left(\frac{S}{S_{min}}\right)^{-\frac{2r}{\sigma^2}} N\left(-a_1 + \frac{2r}{\sigma}\sqrt{T}\right) - e^{rT}N(-a_1) \right)$$

$$a_1 = \frac{\ln\left(\frac{S}{S_{min}}\right) + \left(r + \frac{1}{2}\sigma^2\right)T}{\sigma\sqrt{T}}$$

$$a_2 = a_1 - \sigma\sqrt{T}$$

6.3. Comparison between Monte Carlo Simulations and Analytical Results

Given lookback options as an example (see **Table 3**), the discrepancies in pricing across different volatilities and strikes are noticeable. The analytical results typically provide smoother and more consistent pricing as compared to the Monte Carlo results, which can show greater variance due to the stochastic nature of the simulation process.

For Lookback options, both methods affirm that higher volatility significantly increases the pricing of these options. This effect is more pronounced in the Monte Carlo simulations, where increased variability in simulated asset paths leads to a wider distribution of potential maximum and minimum values, thus enhancing the value of Lookback options which benefit from extreme price movements. For example, in the analytical results, a Lookback call option with a strike of 95 and volatility $\sigma = 0.8$ is priced at approximately 83.94, while the Monte Carlo simulation shows a higher price of about 98.46. This difference suggests that Monte Carlo simulations may capture market extremes more effectively in

certain conditions, possibly due to the method's ability to model a broader range of market scenarios than the typical assumptions underlying analytical formulas.

Moreover, for floating strike options, the Monte Carlo method shows significantly higher prices at higher volatility levels compared to the analytical model, which can be attributed to the dynamic adaptation of the strike price to the optimal historical price during the option's life. For instance, at $\sigma = 1.0$ and $K = 100$, the floating strike Lookback call option is priced at about 84.82 analytically, versus 98.43 in the simulation. This indicates that Monte Carlo simulations might offer a more realistic depiction of pricing under extreme market conditions, which are not as conservatively estimated by analytical solutions.

Therefore, while both pricing methods validate the fundamental behavior expected of Lookback options under varying market conditions, the Monte Carlo simulations appear to provide a more robust reflection of market dynamics, especially in higher volatility environments. This could be crucial for financial modeling and risk management, as it highlights the potential underestimation of risk when relying solely on analytical solutions in highly volatile or unpredictable markets.

Analytical Solutions for Lookback Options					Monte Carlo Results	
Type	**Sigma**	**Strike**	**Call Price**	**Put Price**	**Call Price**	**Put Price**
Fixed Strike	0.2	95	23.45	21.66	23.13	7.73
		100	13.24	14.98	18.48	11.74
		105	47.65	15.43	14.35	16.70
	0.5	95	114.92	8.22	47.81	25.08
		100	9.83	0.00	45.53	30.02
		105	66.83	4.88	42.28	34.48
	0.8	95	83.94	52.90	83.39	38.55
		100	35.52	1.51	77.05	43.43
		105	35.02	55.05	73.44	48.90
Floating Strike	0.2	95	20.12	16.36	17.28	14.03
		100	11.91	25.96	16.67	13.76
		105	37.89	16.79	16.20	13.39
	0.5	95	31.82	39.95	33.03	41.19
		100	37.88	77.46	33.04	41.81
		105	44.57	50.53	32.85	42.45
	0.8	95	48.70	135.33	38.55	72.19
		100	80.84	221.21	43.43	72.10
		105	7.51	96.59	48.90	71.97

Table 3 – Analytical Pricing Solutions for Lookback Options

7. Extension II: Uncertain Volatility Modelling for Lookback Options

With the development of stochastic theory in quantitative finance for volatility modelling, a lot of researches have been focusing on probability theory. The premise of applying probability theory is that the probability distribution has to be close enough to the real frequency. However, in real world, especially in markets experiencing significant uncertainty or lack of sufficient data, the assumption and probabilistic approach may not hold. Therefore, uncertainty theory has been introduced to quantify belief degrees for any indeterminate event. The process operates without the need for predefined probability distributions.

Wilmott (2007) has mentioned that it is normal to give ranges for the future values of uncertain parameters while valuing options with uncertain parameters. For volatility, this means that the assumption is made such that the volatility at a given time spot will fall within the below range:

$$\sigma^- < \sigma < \sigma^+$$

However, the challenge remains in accurately estimating the boundary volatility at a specific time or over a designated period. Liu (2007) introduced a robust framework for modelling dynamics driven by human uncertainty, rather than randomness. Liu (2007) and Liu (2015) introduced uncertain differential equations which are defined by the canonical Liu process, which is a counterpart to the Brownian motion in stochastic calculus but designed for handling uncertainty. The uncertain volatility model can be defined as below:

$$dS_t = \mu S_t dt + \sqrt{\sigma_t} d\mathcal{L}_{1,t}$$

$$d\sigma_t = \kappa(\theta - \sigma_t)dt + \xi\sqrt{\sigma_t} d\mathcal{L}_{2,t}$$

κ, θ, ξ are parameters of the volatility process just like Heston model. κ represents the rate of mean reversion, θ is the long term mean volatility, and ξ is the volatility of the volatility.

A Liu process $\mathcal{L}_t$ is characterized by several key properties: it starts from zero, has independent and stationary increments, and each increment is a normal uncertain variable with an expected uncertainty measure (not an expected value in the probabilistic sense) of zero and a variance proportional to the time increment squared (Liu 2007). These properties allow the Liu process to effectively model the uncertain dynamics observed in financial markets, particularly in the context of volatility. Note that $d\mathcal{L}_{1,t}, d\mathcal{L}_{2,t}$ are just two independent processes.

The numerical method employed in this analysis is Monte Carlo simulations. This section will detail two distinct approaches to simulating uncertain volatility models for pricing lookback options. Asian options are not discussed due to their averaging characteristic, which, as demonstrated by the results above, leads to reduced sensitivity to volatility compared to lookback options.

7.1. Parametric Uncertain Volatility Estimation

Yao and Chen (2013) and Liu (2015) have defined and presented formulas to solve uncertain differential equations numerically which establishes the relation between uncertain differential equation and ordinary differential equation. From their research, uncertain increments driven by Liu process $d\mathcal{L}_t$ can be approximated in a deterministic form using the inverse uncertainty distribution function of the confidence level α:

$$d\mathcal{L}_t \approx \psi^{-1}(\alpha)dt$$

This $\psi^{-1}(\alpha)$ often takes the form of a normalized constant times a function of α, to be consistent with the research from Yao and Chen (2013), Liu (2007) and Liu (2015), this project uses their approximation of function $\psi^{-1}(\alpha)$:

$$\psi^{-1}(\alpha) = \frac{\sqrt{3}}{\pi}\ln\frac{\alpha}{1-\alpha}$$

Therefore, Liu (2007) suggests that the corresponding uncertain stock price paths can be rewritten as:

$$dS_t^\alpha = \mu S_t^\alpha dt + \frac{\sqrt{3}}{\pi} S_t^\alpha \sqrt{\sigma_t^\alpha}\ln\frac{\alpha}{1-\alpha}dt$$

This is just an ordinary differential equation, and it can be solved by following the below steps:

$$\frac{dS_t^\alpha}{S_t^\alpha} = \mu dt + \frac{\sqrt{3}}{\pi}\sqrt{\sigma_t^\alpha}\ln\frac{\alpha}{1-\alpha}dt$$

$$\int_0^t \frac{1}{S_s^\alpha} dS_s^\alpha = \int_0^t \mu\, ds + \frac{\sqrt{3}}{\pi}\ln\frac{\alpha}{1-\alpha}\int_0^t \sqrt{\sigma_s^\alpha}\, ds$$

$$\ln S_t^\alpha - \ln S_0^\alpha = \mu dt + \frac{\sqrt{3}}{\pi}\ln\frac{\alpha}{1-\alpha}\int_0^t \sqrt{\sigma_s^\alpha}\, ds$$

$$S_t^\alpha = S_0^\alpha \exp\left\{dt + \frac{\sqrt{3}}{\pi}\ln\frac{\alpha}{1-\alpha}\int_0^t \sqrt{\sigma_s^\alpha}\, ds\right\}$$

Similarly, the corresponding uncertain volatility follows the below ordinary differential equation:

$$d\sigma_s^\alpha = \kappa(\theta - \sigma_s^\alpha)ds + \frac{\sqrt{3}}{\pi}\sigma\sqrt{\sigma_s^\alpha}\ln\frac{\alpha}{1-\alpha}ds$$

The Monte Carlo simulation in the algorithm for the above processes is captured under <class UncertainVolI>. The parameters for volatility process are selected based on the empirical research being conducted by Liu (2007) for the scenarios of implied volatility being around 0.2, which are: $\kappa =$

$0.3, \theta = 0.2, \xi = 0.1$. Since the long-term mean reverting volatility is selected as 0.2, only the options with volatility configuration of 0.2 priced in the previous section will be compared and discussed here.

The **Figure 8** presents the result of the uncertain volatility estimation. However, it does not seem to match the volatility dynamics of the reality.

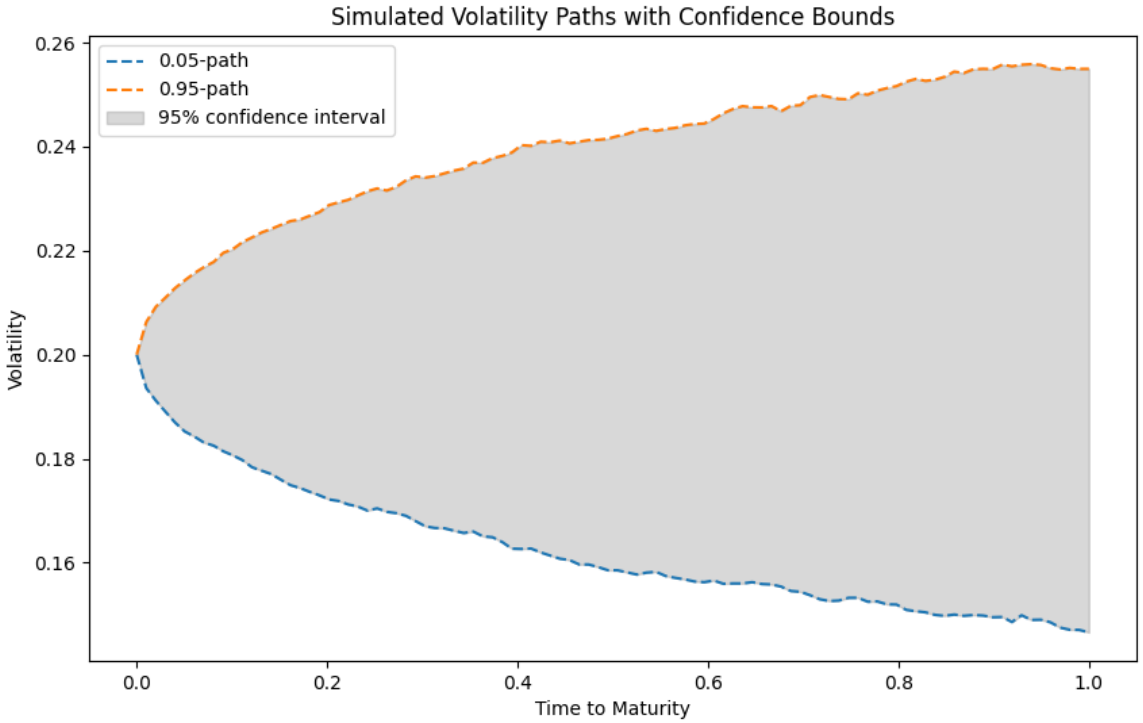

Figure 8 – Parametric Uncertain Volatility Estimates

7.2. Non-Parametric Uncertain Volatility Simulation

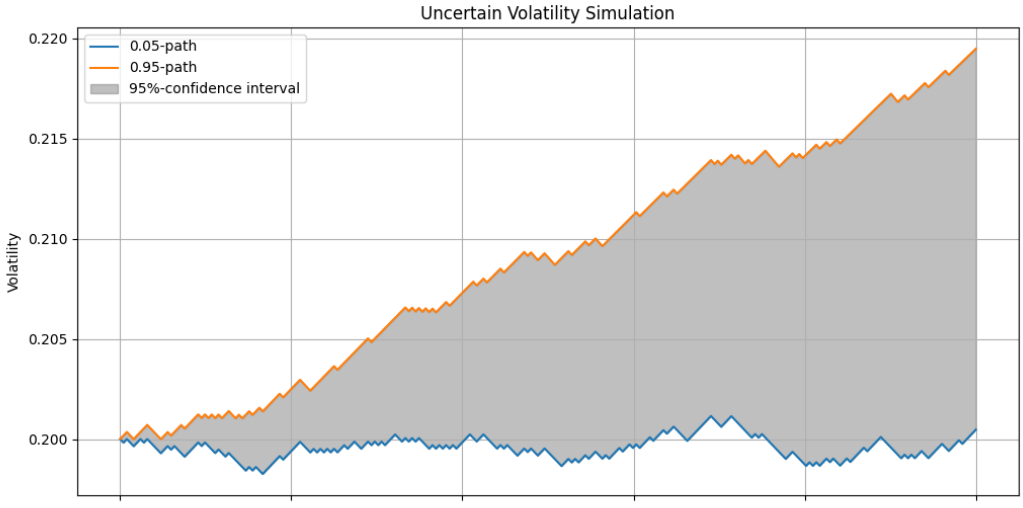

Figure 9 – Non parametric Uncertain Volatility Estimates

The generalized uncertain volatility is estimated from the definition of Liu process (2007) instead of trying to transform the uncertain differential equations into ordinary differential equations. The simulation process starts by simulating Liu process increments directly, which handle uncertainties in model parameters and external influences, allowing for the generation of volatility paths with specified confidence intervals (e.g., 0.05 and 0.95 paths). In comparison to the parametric method described in the academic paper where volatility is modeled using a deterministic parametric function leading to a specific distribution of outcomes, the algorithm provided here uses a non-parametric approach.

Specifically, the parametric method utilizes a formula above involving as a scaling factor in the transformation of uncertainty into variability over time, representing a more mathematically structured approach to modeling the behavior of volatility. Contrastingly, the algorithm <class UncertainVol2> applies a simulation-based methodology allowing for a dynamic and flexible representation of volatility over time without assuming any specific parametric form or distribution, adapting to varying market conditions and reflecting a broader range of potential outcomes. This results in a model that potentially captures more complex behaviors of market volatility and provides pricing that reflects a higher degree of uncertainty.

7.3. Simulation Results

Lookback Option under Uncertain Volatility						
Strike Type	**Option Type**	**Strike**	**UV_1**	**UV_2**	**Monte Carlo**	**Analytical**
Fixed	Call	95	22.64	7.54	23.13	23.45
	Call	100	17.74	11.48	18.48	13.24
	Call	105	13.69	0.01	14.35	47.65
	Put	95	7.45	1.48	7.73	21.66
	Put	100	11.41	1.20	11.74	14.98
	Put	105	16.04	21.59	16.70	15.43
Floating	Call	95	16.41	5.66	17.28	20.12
	Call	100	16.03	0.08	16.67	11.91
	Call	105	16.33	8.87	16.20	37.89
	Put	95	12.86	2.01	14.03	16.36
	Put	100	13.11	8.86	13.76	25.96
	Put	105	12.82	0.23	13.39	16.79

Table 4 – Lookback Option Pricing under Uncertain Volatility

Table 4 presents the outcomes of pricing lookback options under an uncertain volatility model, assuming an initial volatility $\sigma = 0.2$. The table further facilitates a comparison between the prices from uncertain volatility models and prices from Monte Carlo simulation as well as analytical solution at this volatility level. It is apparent that the results derived from the second uncertain volatility model (the generalized model discussed in Section 7.2) do not seem to be correct. These results do not align with the theoretical

properties of lookback options and exhibit significant deviations from both Monte Carlo and analytical solutions. In contrast, the first uncertain volatility model, outlined in Section 7.1, demonstrates proficiency in pricing lookback options, showing minimal deviation from the Monte Carlo simulations. However, a major limitation of this model is its exclusion of possible extreme events, since no probability distributions are taken into account. This omission likely accounts for the close alignment of the results with those of the Monte Carlo simulations under a constant volatility assumption. Moreover, this alignment indirectly validates the accuracy and efficiency of Monte Carlo methods in pricing lookback options, or path-dependent exotic options in general.

8. Conclusion

To conclude, this research has systematically evaluated the efficacy of Monte Carlo simulations in pricing Asian and Lookback options, offering a detailed comparison to traditional analytical methods across various market conditions. It also provides an in-depth analysis of the impact of volatility, strike price variations, and uncertainty volatility modeling on the pricing of Asian and Lookback options.

The findings confirm that volatility significantly influences the pricing of these options, with higher volatility leading to increased option prices due to the greater likelihood of achieving favorable conditions for option execution. This effect is more pronounced in Monte Carlo simulations, which tend to capture the extremes of market behavior more effectively than analytical models.

The study also highlights the differential impact of fixed and floating strike prices on option valuation. Fixed strike options demonstrate higher sensitivity to changes in the underlying asset's price, particularly as the asset price approaches and exceeds the strike price. In contrast, floating strike options show a more stable pricing behavior, adjusting dynamically to the most favorable historical price, which often results in a lower and more predictable pricing structure across varying market conditions.

Additionally, the findings also underscore the superior adaptability of Monte Carlo simulations to complex market dynamics and complex nature of high dimensional path dependent derivative products like Asian and lookback options, particularly in scenarios characterized by high volatility. Notably, the simulations consistently showcased a more pronounced sensitivity to volatility changes, which in turn provided a more dynamic range of pricing outcomes compared to the often static and conservative estimates produced by analytical models. Furthermore, the analysis of standard errors and the stability of prices across multiple simulation runs has affirmed the reliability of Monte Carlo methods. These results further validate the accuracy and practicability of Monte Carlo simulations, even though it has a drawback of being computationally intensive.

Last but not least, by incorporating advanced uncertainty modeling techniques—both parametric and non-parametric—this study has illuminated the significant impact of volatility assumptions on option pricing. The application of these techniques revealed that Monte Carlo simulations not only reflect a

broader spectrum of market possibilities but also enhance the robustness of financial models against the unpredictable nature of financial markets.

In summary, this research validates the strategic advantage of Monte Carlo simulations in financial modeling, advocating for their broader application in the valuation of complex financial instruments. It paves the way for further exploration into hybrid modeling approaches that could potentially bridge the gap between theoretical accuracy and practical applicability in financial markets.

9. References

Ahmad, R. (2024). Exotic options lecture [PowerPoint slides]. CQF (Certificate in Quantitative Finance), January 2024 Cohort.

Haug, E. G. (2007). *Option pricing formulas*. McGraw-Hill Professional.

Kwok, Y.-K. (2008). *Mathematical models of financial derivatives (2nd ed.)*. Springer Finance.

Liu B (2014) Uncertainty distribution and independence of uncertain processes. Fuzzy Optim Decis Mak 13(3):259–271.

Liu B (2015) *Uncertainty Theory*, 5th edn. Uncertainty Theory Laboratory.

Musiała, M., & Rutkowski, M. (2009). *Stochastic modelling and applied probability. (2nd ed.)*. Springer-Verlag Berlin Heidelberg. DOI: 10.1007/978-3-540-26653-2.

Wilmott, P. (2007). *Paul Wilmott on Quantitative Finance*, Volume 2. John Wiley & Sons.

Wilmott, P. (2007). *Paul Wilmott on Quantitative Finance*, Volume 3. John Wiley & Sons.

Yao K , Chen X . *A numerical method for solving uncertain differential equations*. J Intell Fuzzy Syst 2013;25(3):825–32 .

10. Appendices

Appendix A – Solution of SDE dS_t

We start by solving the above stochastic differential equation. Let $Y_t = \ln(S_t)$, by Itô's lemma, which is usually used to find the differential of a function of a stochastic process, we have:

$$dY_t = \frac{\partial Y_t}{\partial S_t} dS_t + \frac{1}{2} \frac{\partial^2 Y_t}{\partial S_t^2} (dS_t)^2$$

Knowing that

$$\frac{\partial Y_t}{\partial S_t} = \frac{1}{S_t}, \frac{\partial^2 Y_t}{\partial S_t^2} = -\frac{1}{S_t^2}$$

Additionally, we can extend $(dS_t)^2$:

$$(dS_t)^2 = \left(\mu S_t dt + \sigma S_t dW_t^{\mathbb{P}}\right)^2$$

$$= (\mu S_t dt)^2 + \left(\sigma S_t dW_t^{\mathbb{P}}\right)^2 + 2(\mu S_t dt)\left(\sigma S_t dW_t^{\mathbb{P}}\right)$$

By applying Itô's properties: $(dt)^2 = 0, dt \times dW_t^{\mathcal{F}} = 0, \lim_{dt \to 0} \left(dW_t^{\mathbb{P}}\right)^2 = dt$:

$$(dS_t)^2 = \left(\sigma S_t dW_t^{\mathbb{P}}\right)^2 = \sigma^2 S_t^2 dt$$

Substitute all back to dY_t:

$$dY_t = \frac{1}{S_t}\left(\mu S_t dt + \sigma S_t dW_t^{\mathbb{P}}\right) - \frac{1}{2}\frac{1}{S_t^2}(\sigma^2 S_t^2 dt)$$

$$= \mu dt + \sigma dW_t^{\mathbb{P}} - \frac{1}{2}\sigma^2 dt = \left(\mu - \frac{1}{2}\sigma^2\right) dt + \sigma dW_t^{\mathbb{P}}$$

Afterwards, we integrate both sides over the interval from 0 to t:

$$\int_0^t dY_s = \int_0^t \left(\mu - \frac{1}{2}\sigma^2\right) ds + \int_0^t \sigma dW_t^{\mathbb{P}}$$

This gives us:

$$Y_t - Y_0 = \left(\mu - \frac{1}{2}\sigma^2\right)(t - 0) + \sigma\left(W_t^{\mathbb{P}} - W_0^{\mathbb{P}}\right) = \left(\mu - \frac{1}{2}\sigma^2\right) t + \sigma W_t^{\mathbb{P}}$$

Note that $W_0^{\mathbb{P}} = 0$, this is because one of the properties of a Wiener process or Brownian motion: it starts at zero with probability one.

Since $Y_t = \ln(S_t)$, and $Y_0 = \ln(S_0)$, we can rewrite the above equation as:

$$\ln(S_t) - \ln(S_0) = \left(\mu - \frac{1}{2}\sigma^2\right)t + \sigma W_t^{\mathbb{P}}$$

Therefore:

$$\ln(S_t) = \ln(S_0) + \left(\mu - \frac{1}{2}\sigma^2\right)t + \sigma W_t^{\mathbb{P}}$$

$$S_t = e^{\ln(S_0)+\left(\mu-\frac{1}{2}\sigma^2\right)t+\sigma W_t^{\mathcal{F}}} = e^{\ln(S_0)}e^{\left(\mu-\frac{1}{2}\sigma^2\right)t+\sigma W_t^{\mathcal{F}}} = S_0 e^{\left(\mu-\frac{1}{2}\sigma^2\right)t+\sigma W_t^{\mathbb{P}}}$$

Appendix B – Proof of Girsanov Theorem

Recall the basic Brownian motion properties: $W_0^{\mathbb{Q}} = 0$ and $W_t^{\mathbb{Q}}$ is continuous. Let's write $dW_t^{\mathbb{Q}}$ in the below way:

$$dW_t^{\mathbb{Q}} = dW_t^{\mathbb{P}} + \theta_t dt$$

$$dW_t^{\mathbb{Q}} dW_t^{\mathbb{Q}} = \left(dW_t^{\mathbb{P}} + \theta_t dt\right)^2 = \left(dW_t^{\mathbb{P}}\right)^2 + (\theta_t dt)^2 + 2\theta_t dW_t^{\mathbb{P}} dt = dt$$

Aligning with what has defined by Shreve (2004), $W_t^{\mathbb{P}}$ is a Brownian motion on probability space $(\Omega, \mathcal{F}, \mathbb{P})$. $\mathcal{F}(t)$ is a filtration associated with $W_t^{\mathbb{P}}$, and θ_t is an adapted process, and $0 \le t \le T$.

Let's start by proving Λ_t is a martingale:

$$\Lambda_t = \exp\left\{-\int_0^t \theta_s \, dW_s^{\mathbb{P}} - \frac{1}{2}\int_0^t \theta_s^2 \, ds\right\}$$

Let $f(x) = e^x$, $X_t = -\int_0^t \theta_s \, dW_s^{\mathbb{P}} - \frac{1}{2}\int_0^t \theta_s^2 \, ds$. It is easy to obtain:

$$\frac{df(x)}{dx} = e^x = \frac{d^2 f(x)}{dx^2}$$

As a result, by applying Itô's formula:

$$d\Lambda_t = df(X_t) = \frac{df(X_t)}{dX_t} dX_t + \frac{1}{2}\frac{d^2 f(X_t)}{dX_t^2}(dX_t)^2$$

$$dX_t = d\left(-\int_0^t \theta_s \, dW_s^{\mathbb{P}} - \frac{1}{2}\int_0^t \theta_s^2 \, ds\right) = -\theta_t dW_t^{\mathbb{P}} - \frac{1}{2}\theta_t^2 dt$$

Therefore:

$$d\Lambda_t = e^{X_t}\left(-\theta_t dW_t^{\mathbb{P}} - \frac{1}{2}\theta_t^2 dt\right) + \frac{1}{2}e^{X_t}\left(-\theta_t dW_t^{\mathbb{P}} - \frac{1}{2}\theta_t^2 dt\right)^2$$

$$= e^{X_t}\left(-\theta_t dW_t^{\mathbb{P}} - \frac{1}{2}\theta_t^2 dt\right) + \frac{1}{2}e^{X_t}\theta_t^2 dt = -e^{X_t}\theta_t dW_t^{\mathbb{P}} = -\Lambda_t \theta_t dW_t^{\mathbb{P}}$$

Rewrite it in integral form:

$$\Lambda_t = \Lambda_0 - \int_0^t \theta_u \Lambda_u dW_u^{\mathbb{P}}$$

$$\Lambda_t = \mathbb{E}[\Lambda_T | \mathcal{F}_t] = \mathbb{E}[\Lambda | \mathcal{F}_t]$$

Λ_t is also called a Radon-Nikodym process. Now, let's consider the differential of the product of Brownian motion $W_t^{\mathbb{Q}}$ under new probability measure $\mathbb{Q}$ and the Radon-Nikodym process. By Itô's product rule, the following equation can be obtained:

$$d\left(W_t^{\mathbb{Q}}\Lambda_t\right) = W_t^{\mathbb{Q}}d\Lambda_t + \Lambda_t dW_t^{\mathbb{Q}} + dW_t^{\mathbb{Q}}d\Lambda_t$$

Substitute $d\Lambda_t$ back in:

$$\begin{aligned} d\left(W_t^{\mathbb{Q}}\Lambda_t\right) &= -W_t^{\mathbb{Q}}\Lambda_t\theta_t dW_t^{\mathbb{P}} + \Lambda_t\left(dW_t^{\mathbb{P}} + \theta_t dt\right) - \left(dW_t^{\mathbb{P}} + \theta_t dt\right)\left(\Lambda_t\theta_t dW_t^{\mathbb{P}}\right) \\ &= -W_t^{\mathbb{Q}}\Lambda_t\theta_t dW_t^{\mathbb{P}} + \Lambda_t dW_t^{\mathbb{P}} + \Lambda_t\theta_t dt - \Lambda_t\theta_t\left(dW_t^{\mathbb{P}}\right)^2 + \Lambda_t\theta_t^2 dW_t^{\mathbb{P}}dt \\ &= -W_t^{\mathbb{Q}}\Lambda_t\theta_t dW_t^{\mathbb{P}} + \Lambda_t dW_t^{\mathbb{P}} + \Lambda_t\theta_t dt - \Lambda_t\theta_t dt + 0 \\ &= -W_t^{\mathbb{Q}}\Lambda_t\theta_t dW_t^{\mathbb{P}} + \Lambda_t dW_t^{\mathbb{P}} = \left(-W_t^{\mathbb{Q}}\theta_t + 1\right)\Lambda_t dW_t^{\mathbb{P}} \end{aligned}$$

Therefore $\left(W_t^{\mathbb{Q}}\Lambda_t\right)$ is a Itô's integral:

$$W_t^{\mathbb{Q}}\Lambda_t = \int_0^t \left(-W_t^{\mathbb{Q}}\theta_t + 1\right)\Lambda_t dW_t^{\mathbb{P}}$$

As a result, $\left\{W_t^{\mathbb{Q}}\Lambda_t\right\}$ is a Martingale.

For any given s which falls in the interval: $0 \le s \le t \le T$:

$$\mathbb{E}^{\mathbb{Q}}\left[W_t^{\mathbb{Q}}|\mathcal{F}_s\right] = \frac{1}{\Lambda_s}\mathbb{E}\left[W_t^{\mathbb{Q}}\Lambda_t|\mathcal{F}_s\right] = \frac{1}{\Lambda_s}W_s^{\mathbb{Q}}\Lambda_t = W_s^{\mathbb{Q}}$$

Therefore, $\left\{W_t^{\mathbb{Q}}\right\}$ is a Martingale.

Appendix C – Convergence of $\sqrt{\Delta t}Z$ to a continuous Wiener Process

Apply Central Limit Theorem proving the discretization $\sqrt{\Delta t}Z$ will converge into a continuous Wiener process:

The Central Limit Theorem (CLT) in a foundational result in probability theory that explains why many distributions tend to be close to the normal distribution, particularly when a large number of small, random variables are added together. This section will mathematically demonstrate how this applies to the convergence of S_n to a normally distributed random variable as $n \to \infty$, which represents the continuous time Wiener process.

$$S_n = \sqrt{T}\frac{1}{\sqrt{n}}\sum_{i=1}^{n} Z_i$$

Note that Z_i are independent and identically distributed random variables with a standard normal distribution, so they have a mean $\mu = 0$ and variance $\sigma^2 = 1$. Δt is the time increment in the discretized process so that $\Delta t = \frac{T}{n}$, where T is the fixed end time. Additionally, note that W_T is the value of the Wiener Process at time T, which has a $N(0, T)$ distribution.

First of all, we need to standardize S_n to apply the Central Limit Theorem. Known that the variance of each Z_i is 1, so the variance of the sum $\sum Z_i$ is n. This is because variances of independent random variables add up. Therefore, the standard deviation of the sum is $\sqrt{n}$.

The CLT states that if $X_1, X_2, \dots, X_n$ are i.i.d random variables with mean μ and variance σ^2, then their normalized sum converges in distribution to a standard normal distribution as $n \to \infty$.

$$\frac{1}{\sigma\sqrt{n}}\sum_{i=1}^{n}(X_i - \mu) \xrightarrow{d} \mathcal{N}(0,1)$$

Since Z_i are already standardized with $\mu = 0, \sigma^2 = 1$, we can apply this directly:

$$\frac{1}{\sqrt{n}}\sum_{i=1}^{n} Z_i \xrightarrow{d} \mathcal{N}(0,1)$$

Multiplying both sides by $\sqrt{T}$:

$$\sqrt{T}\frac{1}{\sqrt{n}}\sum_{i=1}^{n} Z_i \xrightarrow{d} \mathcal{N}\left(0, \sqrt{T}^2\right)$$

Since $\sqrt{T}\frac{\sum_{i=1}^{n} Z_i}{\sqrt{n}} = S_n$, and the above equation shows that it converges in distribution to $\mathcal{N}(0, T)$, which matches the distribution of W_T. As a result, we have:

$$S_n = \sqrt{T}\frac{1}{\sqrt{n}}\sum_{i=1}^{n} Z_i \xrightarrow{d} \mathcal{N}(0,T)$$

Note that $\xrightarrow{d}$ signifies converges in distribution. This means that as n becomes very large, the distribution of the left-hand side of the expression will become closer and closer to the distribution on the right-hand side of the expression

In conclusion, this shows that as n increases, the discretized sum S_n becomes a better approximation to the continuous Wiener process at time T, converging in distribution to the same normal distribution as W_T. This result justifies the use of the Euler-Maruyama method for discretizing continuous SDES and approximating them by a Wiener process.

Appendix D – Proof of Convergence: Discrete Period Sampled Averages to continuous Sampled Averages (Asian Optioins)

In arithmetic averaging, to show how the discrete average approximates the continuous average as the number of intervals n increases, we construct the below steps:

First, we define Riemann Sum: The Riemann sum for a function $f(t)$ over an interval $[a, b]$ with n subintervals is given by:

$$S_n = \sum_{i=1}^{n} f(t_i^*)\,\Delta t$$

$$\Delta t = \frac{b-a}{n}$$

t_i^* denotes the sample point in the i^{th} subinterval.

Let $f(t) = S_t$, the asset price at time t, we can divide interval $[0, T]$ into n subintervals, each of length $\Delta t = \frac{T}{n}$. Choose $t_i^* = t_i = \frac{iT}{n}$ corresponding to the end of each interval.

Now the discrete sum can be written as Riemann Sum:

$$\frac{1}{n}\sum_{i=1}^{n} S_{t_i} \to \frac{T}{n}\sum_{i=1}^{n}\frac{1}{T}S_{t_i} = \sum_{i=1}^{n}\frac{\Delta t}{T}S_{t_i}$$

This is a Riemann sum approximation of $\frac{1}{T}\int_0^T S_t\,dt$. As $n \to \infty$, $\Delta t \to 0$, and by definition of the integral as the limit of Riemann sums:

$$\lim_{n\to\infty}\frac{1}{n}\sum_{i=1}^{n} S_{t_i} = \frac{1}{T}\int_0^T S_t\,dt$$

In geometric averaging, the transition from discrete to continuous requires dealing with the logarithms of the prices. We start by defining the discrete geometric averaging:

$$A_t = \left(\prod_{i=1}^{n} S_{t_i} \right)^{\frac{1}{n}}$$

We can natural logarithms on both sides:

$$\ln A_t = \frac{1}{n} \sum_{i=1}^{n} \ln S_{t_i}$$

Similar to the steps under arithmetic averaging, we consider $\Delta t = \frac{T}{n}$, as a result:

$$\frac{1}{n} \sum_{i=1}^{n} \ln S_{t_i} = \frac{T}{n} \sum_{i=1}^{n} \frac{1}{T} \ln S_{t_i}$$

Similarly, this is a Riemann sum approximation of $\frac{1}{T} \int_0^T \ln S_t \, dt$. Now as $n \to \infty$, the below convergence holds:

$$\lim_{n \to \infty} \frac{1}{n} \sum_{i=1}^{n} \ln S_{t_i} = \frac{1}{T} \int_0^T \ln S_t \, dt$$

Now if we exponentiate both sides:

$$e^{\ln A_t} = e^{\frac{1}{T} \int_0^T \ln S_t dt} = A_t$$

As a result, we have defined our continuously monitored geometric averaging form as:

$$A_t = \exp \left\{ \frac{1}{t} \int_0^t \ln S_u \, du \right\}$$

Appendix E - Covariance of Brownian Motion Increments

Brownian motion W_t is a stochastic process characterized by several key properties:

1. $Z_0 = 0$, unless being defined with a different initial condition
2. Independent increments: The increments $W_u - W_v$ is independent of the process before v for $u > v$
3. Stationary increments: The distribution $W_u - W_v$ depends only on the difference $u - v$, and this increment is normally distributed with mean 0 and variance $u - v$.
4. The paths of W_t are almost surely continuous.

For any two times u, v where $t \leq v \leq u$, consider the increments $W_u - W_t$ and $W_v - W_t$, by definition:

$$W_u - W_t = (W_u - W_v) + (W_v - W_t)$$

Since $(W_v - W_t)$ is part of both increments $W_u - W_v$ and $W_v - W_t$, the overlapping portion contributes to their covariance.

By definition, the covariance of two random variables X, Y is given by:

$$Cov(X, Y) = \mathbb{E}[XY] - \mathbb{E}[X]\mathbb{E}[Y]$$

For Brownian motion increments:

$$\mathbb{E}[W_u - W_t] = \mathbb{E}[W_v - W_t] = 0$$

The covariance simplifies to:

$$Cov(W_u - W_t, W_v - W_t) = \mathbb{E}[(W_u - W_t)(W_v - W_t)]$$

Considering $v \leq u$:

$$W_u - W_t = (W_u - W_v) + (W_v - W_t)$$

$$(W_u - W_t)(W_v - W_t) = (W_u - W_t)(W_v - W_t) + (W_v - W_t)^2$$

Since $W_u - W_t$ is independent of $W_v - W_t$, the expectation of the first term becomes 0, therefore:

$$\mathbb{E}[(W_u - W_t)(W_v - W_t)] = \mathbb{E}[(W_v - W_t)^2] = \mathbb{V}ar(W_v - W_t) = v - t$$

This holders generally, where $v \leq u$. If $u < v$, swap the roles of u, v, hence, the covariance is:

$$Cov(W_u - W_t, W_v - W_t) = \min(u, v) - t$$